Conservation of molecular responses upon viral infection in the non-vascular plant *Marchantia polymorpha*

Eric Moner-Ros[1*], Tamara Jiménez-Góngora[1*], Luis Villar-Martín[1], Víctor M. González-Miguel[2], Denis Kutnjak[3] and Ignacio Rubio-Somoza[1,4,]

[1]Molecular Reprogramming and Evolution (MoRE) Laboratory, Centre for Research in Agricultural Genomics (CRAG), CSIC-IRTA-UAB-UB, Campus UAB-Edifci CRAG. 08193 Cerdanyola del Vallés, Spain.

[2]Data Analysis area, Bioinformatics Core Unit, Centre for Research in Agricultural Genomics (CRAG), CSIC-IRTA-UAB-UB, Campus UAB-Edifci CRAG. 08193 Cerdanyola del Vallés, Spain.

[3]National Institute of Biology, Department of Biotechnology and Systems Biology, Ljubljana, Slovenia.

[4]Consejo Superior de Investigaciones Científicas (CSIC), Barcelona 08001, Spain.

*Those authors contributed equally to this work

To whom correspondence should be addressed: Ignacio.rubio@cragenomica.es

Abstract

After their transition from water to land around 450 million years ago, plants colonized new habitats facing unprecedented pathogenic microbes. That expansion was mostly supported by a growing anatomical complexity based on the acquisition of developmental innovations, such as roots, stomata and vascular tissue. Despite several of those innovations became central for the interaction between plants and their associated microbes, little is known about their impact on plant immune programs and on the diversification of infection strategies of their pathogens. A paradigmatic case is the close relationship between plant vasculature and viruses. Vascular tissues provide a unique cellular environment for viral replication and existence, besides constituting a fast track for viral systemic spread throughout the plant. Since most of our knowledge about plant-virus interactions come from studies in vascular plants, we here present a comparative study to contribute to the understanding of the evolution of plant-virus interactions by molecularly characterizing the interplay between the bryophyte Marchantia polymorpha and viruses. Virome analysis of Marchantia plants shows that they are primarily associated with RNA viruses in natural settings. Additional molecular characterization of the interaction between Marchantia and tobacco mosaic virus (TMV) show conserved basic

processes with vascular plants and divergent features. Viral infection triggers an extensive transcriptional reprogramming in Marchantia encompassing broad range defence responses, inhibition of cell cycle and photosynthesis and a sustained wound response that prevents further viral movement. Additionally, infected plants show premature aging and organ maturation. Notably, we found that some core responses that occur in infected areas in Marchantia, were described to be restricted to vascular tissues in Nicotiana, suggesting that evolutionary appearance of developmental innovations that became central in plants-virus interactions resulted in re-routing of defence responses. Finally, we uncover the conserved role of a transcription factor interacting with the TMV silencing suppressor p126 in specifically abrogating TMV infection.

Introduction

It is estimated that plants developed a functional vascular system through repurposing of preexisting genes around 420 million years ago, which facilitated the growth of larger plants by providing mechanical support and enabling long distant transport of water, nutrients, and signalling molecules (Bowles et al., 2022, Lucas et al., 2013). Viruses are obligate parasites that can infect virtually any living organism hijacking central host cellular functions to replicate and spread within and intra hosts. Coincidentally with land colonization, the repertoire of viruses (virome) associated to plants enlarged and diversified both in nature and infection strategies. Although our current knowledge lacks information about virome composition at intermediately divergent plant lineages, it appears that viruses with large DNA genomes majorly infecting unicellular chlorophyte algae were displaced by an increasing population of viruses with RNA and small DNA genomes found in vascular plants (Mushegian et al., 2016). Plant vasculature has become central for the success of viral infections in tracheophytes, not only serving as fast track for viral systemic spread, but also providing a unique cellular environment for some viruses which replication is restricted to that tissue (Kappagantu et al., 2020). Accordingly, vascular cells are thought to present specific responses to viral infection when compared to other leaf cell-types (Collum and Culver, 2017).

Our current understanding of the molecular events governing plant-virus interactions is vastly shaped by studies focusing on vascular plants, mainly crops. Plants respond to viral infections via at least three different but interconnected defence mechanisms (Mandadi and Scholthof, 2013).

63 Firstly, plants have an extracellular surveillance system that monitors the presence of pathogens
64 through the recognition of highly conserved microbe patterns dubbed as Pattern-associated
65 molecular patterns (PAMPs), such as viral derived double-strand RNAs (dsRNAS), the bacterial
66 flagellin or the fungal chitin. Detection of those molecules by specialized surface-localized
67 receptor kinases (Pattern recognition receptors, PRRs), triggers a first layer of defence called
68 PAMP-triggered immunity (PTI). PRRs expression is often restricted to focal points for microbial
69 interaction and invasion (Beck et al., 2014, Yotsui et al., 2023). Two additional surveillance
70 mechanisms monitor the intracellular presence of microbe-derived molecules. Highly stable
71 dsRNAs produced by viruses during their life cycle, independently of the DNA or RNA nature of
72 their genomes, are detected by the RNA silencing machinery which constitutes a conserved
73 antiviral defence mechanism both in plants and animals (Ding et al., 2018, Ding and Voinnet,
74 2007). Additionally, RNA silencing machinery also recognizes dsRNA generated from the
75 conversion of exogenous and endogenous single strand RNAs (ssRNA) by RNA-dependent RNA
76 polymerases (RDRs). RDR1 and RDR6 have been involved in antiviral defence in *Arabidopsis*
77 *thaliana* and *Nicotiana tabacum* (Garcia-Ruiz et al., 2010, Rakhshandehroo et al., 2017, Ying et
78 al., 2010), even though *Nicotiana benthamiana* has only a functional RDR6 (Bally et al., 2015).
79 Upon recognition, viral dsRNAs are trimmed in small RNAs (visRNAs) of 20 to 24 nucleotides in
80 length by members of the DICER-like family, mainly DCL2, DCL3 and DCL4 in Arabidopsis and
81 Nicotiana (Garcia-Ruiz et al., 2010, Lewsey and Carr, 2009). The resulting visRNA duplexes are
82 subsequently loaded into proteins from the ARGONAUTE family, which are the core elements of
83 the RNA-induced silencing complex (RiSC), and used to scan the intracellular space for the source
84 of dsRNA precursors in a sequence complementary manner abrogating viral infection (Lopez-
85 Gomollon and Baulcombe, 2022). In turn, viruses produce countermeasures, known as silencing
86 suppressors, targeted to interfere with different steps of the host RNA silencing machinery
87 (Lopez-Gomollon and Baulcombe, 2022). In response to these silencing suppressors, host micro
88 RNAs (miRNA, one of the two main classes of endogenous sRNAs in plants) are no longer
89 functional, allowing the translation of their targets and licensing a new layer of defence. Among
90 the miRNA targets involved in such counter-counter measure, members of the Nucleotide-
91 binding domain leucine-rich repeat (NLR) family are central. Thus, it has been suggested that
92 host miRNAs might work as sensors for the presence of pathogen-derived silencing suppressors
93 enabling a rapid host defence response based on the activation of otherwise silenced miRNA
94 targets (Vasseur et al., 2022). NLRs are core elements of the third intracellular surveillance
95 system for directly monitoring the intracellular presence of pathogen-derived molecules, such

96 as the prototypical case of the tobacco mosaic virus (TMV) replicase by the gene *N* in tobacco
97 (Erickson et al., 1999), or their impact on host cellular homeostasis. NLR-activation triggers the
98 so-called Effector-triggered immunity (ETI), which normally triggers a hypersensitive response
99 (HR) culminating in cell death. Those three defence systems, PTI, RNA silencing and ETI largely
100 rely on the action of the plant hormone Salicylic acid (SA). PTI and ETI responses encompass
101 activation of SA signalling (Pruitt et al., 2021) while SA activates RDR1 in Arabidopsis and
102 Nicotiana (Lee et al., 2016, Ying et al., 2010, Yu et al., 2003). Additionally, RDR1 expression is also
103 induced by treatment with jasmonates (Liu et al., 2009, Xu et al., 2013), another central hormone
104 in plant defence.

105 A Central question in plant-microbe interactions is how the evolution of different plant
106 developmental trajectories, including the acquisition of major innovations, impacts host defence
107 and pathogen infection strategies. In animals, comparative studies have proved very informative
108 about the origin and diversification of their innate immune responses against virus (Iwama and
109 Moran, 2023). Likewise, comparative studies including non-vascular plants, like the liverwort
110 *Marchantia polymorpha*, have been instrumental in understanding the evolution of the
111 interactions between plants and pathogens other than viruses (Carella et al., 2018, Gimenez-
112 Ibanez et al., 2019, Redkar et al., 2022). Incorporating bryophytes into those comparative studies
113 not only provides important information about how plant immune programs may have evolved,
114 but it also bears the potential to determine the contribution of developmental innovations, such
115 as roots, stomata or vasculature, to their diversification.

116 To enable comparative studies towards understanding the evolution of plant-virus interactions,
117 we here present the characterization of the molecular interplay between the non-vascular
118 liverwort *Marchantia polymorpha* and viruses. We firstly defined the composition of the virome
119 of Marchantia plants living in the wild and used that information to select a virus with similar
120 genomic features to those found in nature for further molecular characterization. Additionally,
121 the selected virus should be able to infect a broad range of hosts. Following those criteria, we
122 focused on the first ever isolated virus, the tobacco mosaic virus (TMV). TMV is a ssRNA virus
123 from the Tobamovirus genus that has been extensively used for studying plant-virus interactions
124 in a wealth of plant species, including several Solanaceae species, like tomato and tobacco, and
125 the model plant *Arabidopsis thaliana*, allowing for comparative studies. TMV infects through
126 wound entry points from where it moves cell-to-cell via plasmodesmata, until it reaches the

127 vascular system for systemic infection of distal parts of the plant following the stream of
128 photoassimilates (Liu and Nelson, 2013).

129 Our results show that *Marchantia polymorpha* is associated with RNA viruses in natural
130 populations that can infect lab grown Marchantia plants. Additionally, TMV can replicate in
131 Marchantia plants triggering a conserved transcriptional reprogramming encompassing
132 increased wounding and PTI responses in detriment of photosynthesis and cell cycle progression
133 and leading to aging and senescence. Induction of a wealth of NLR proteins and core elements
134 from the RNA silencing machinery were also observed. Noteworthy, the general response of the
135 RNA silencing machinery observed in Marchantia upon TMV infection is equivalent to that found
136 specifically in vascular tissues of *Nicotiana benthamiana*. We additionally describe a conserved
137 host interactor with the TMV silencing suppressor p126 that triggers cross-species defence
138 against TMV.

139 **Results**

140 ***Marchantia polymorpha* is infected by RNA viruses in nature.**

141 To identify viruses infecting *Marchantia polymorpha* in nature, we performed a virome
142 analysis of a composite plant sample. Marchantia individuals were obtained from three open air
143 botanical gardens throughout Europe: Tübingen (Germany), Bern (Switzerland) and Cambridge
144 (UK). In addition to the expected background of bacteriophage sequences, we detected several
145 known viruses, including some capable of infecting or being associated with plants, fungi or
146 invertebrates (Supplementary table 1). Putatively new virus-like sequences were identified in the
147 dataset, based on i) their relatively high average sequencing depths and ii) similarity to viruses
148 previously associated with plants (Supplementary Table 2). Two previously described and three
149 newly identified viruses were hence selected for further RT-qPCR confirmation of their
150 association with the different *M. polymorpha* individuals, along with plants from the Tak-1
151 reference accession grown in sterile conditions. Specific primers to detect Ligustrum necrotic
152 ringspot virus (LNRV, known to infect plants), Hubei picorna-like virus 51, (detected in a
153 metagenomics study and putatively associated with dragonfly) a newly identified picorna-like
154 virus (which we named Tübingen picorna-like virus 1, with average mapping depth of 2230x and
155 contig length of 7801 nts), a new tombus-like virus (Tübingen tombus-like virus 1, with average
156 mapping depth of 218x and contig length of 4521 nts), and a new sobemo-like virus (Bern
157 sobemo-like virus 1, with average mapping depth of 88x and contig length of 2569 nts) were

158 used for these analysis. While none of those viruses were detected in negative control Tak-1
159 plants, individuals from Tübingen were associated with all tested viruses but the Bern sobemo-
160 like virus 1, which in turn was present in individuals from Bern along with Tübingen picorna-like
161 virus 1. Individuals from the Cambridge population were associated with Hubei picorna-like virus
162 51 and Tübingen picorna-like virus 1 (Supplementary Table 3).

163 Given that Tübingen picorna-like virus 1 was present in all tested populations, we decided to
164 further characterize its genomic features and interaction with *Marchantia polymorpha*. Indeed,
165 Tübingen picorna-like virus 1 had the highest mapping depth of all contigs in our virome analysis
166 and showed a similar genome structure as other unclassified picorna-like viruses (Shi et al.,
167 2016), consisting of two predicted genome open reading frames (ORFs) containing a RNA-
168 dependent RNA polymerase (RdRp) and a coat protein motifs (Figure 1A). Phylogenetic analysis
169 (Figure 1B) of the RdRp protein sequence and its closest NCBI GenBank homologues showed
170 high similarity (80% identity of aligned sequences) of this virus isolate with a recently reported
171 plant associated picorna-like virus (Trichosanthes kirilowii picorna-like virus, QKK82970.1). Much
172 lower identities were observed for Tübingen picorna-like virus 1 (29-42%) and other viruses
173 associated with diverse sources (plants, gastropods, water, crayfish, artropods and bird feces).
174 However, given that they were discovered in metagenomics studies their association with these
175 hosts is only speculative.

176 Next, we tested whether the Tübingen picorna-like virus 1 was able to infect *M. polymorpha* by
177 incubating two-weeks old Tak-1 individuals with extracts isolated from the Tübingen population,
178 which contained the highest levels of Tübingen picorna-like virus 1, as determined by RT-qPCR
179 analysis, or from Tak-1 plants grown in sterile conditions. Individual Marchantia plants were
180 collected one and two weeks after incubation and the levels of viral accumulation were
181 measured by RT-qPCR. Individuals exposed to extracts from infected plants showed a trend of
182 increased viral levels over time, while no amplification was observed in plants incubated with
183 extracts from Tak-1 plants (Figure 1C). This indicated that Tübingen picorna-like virus 1 can
184 replicate in Marchantia.

185 Collectively, those results show that *Marchantia polymorpha* can be infected by RNA viruses in
186 nature.

187 **Tobacco mosaic virus infects *Marchantia polymorpha***

188 Since its identification in the 19th century, tobacco mosaic virus has been extensively used for
189 studying plant-virus interactions in several vascular plant species like Arabidopsis and Nicotiana
190 (Scholthof, 2004). As a first step for comparative studies on plant-virus interactions between
191 vascular and non-vascular plants, we aimed to infect *Marchantia polymorpha* plants with a GFP
192 labelled clone of TMV (Peart et al., 2002). Sap from leaves of healthy and infected *Nicotiana*
193 *benthamiana* plants were isolated and used to incubate two-weeks old Tak-1 plants grown in
194 sterile conditions. After incubation, Marchantia plants were transferred to soil and part of the
195 remaining sap was inoculated mechanically with an abrasive in basal leaves from 1 month old
196 Nicotiana plants, as control for its infectivity. After two weeks, Nicotiana plants showed systemic
197 GFP signal under UV light along with symptoms of infection (Supplementary Figure 1), whereas
198 Tak-1 plants displayed GFP signal in discrete infection foci that increased their size over time
199 (Figure 2A), suggestive of viral replication. This was further corroborated by RT-qPCR
200 amplification of pooled samples of four GFP positive individuals at the first (T1) and second
201 weeks after incubation (T2), in comparison with mock and freshly incubated (T0) plants (Figure
202 2B). Histological sections of the infected area showed presence of the virus in all cell types, as
203 inferred from GFP fluorescence, suggesting no preference for a specific cell-type during viral
204 infection (Figure 2C).

205 Those results confirmed that TMV can infect *M. polymoprha* plants pointing to Marchantia-TMV
206 as a suitable pathosystem for comparative studies.

207 **TMV infection triggers profound molecular reprogramming in *M. polymoprha***

208 To characterize the molecular reprogramming caused by TMV infection, we performed
209 transcriptomic assays. TMV-GFP infected tissue was collected in four pools including 5 plants
210 each, along with the very same area from mock treated plants as control (Supplementary Figure
211 2A). RNA was isolated and the presence of TMV was confirmed by RT-qPCR in each pool
212 (Supplementary Figure 2B). Principal component analysis (PCA, Supplementary Figure 2C) of the
213 transcriptome supported the RT-qPCR results showing a clear separation of infected and mock
214 samples. Since separation among infected samples correlated with viral RT-qPCR levels, we
215 selected the three replicates that had the highest levels of TMV and clustered together for
216 further analysis. A total of 1879 genes were found to be up regulated while 1645 were reduced
217 (padjust<0.05, Log2(fold-change) =1) in response to TMV infection (Supplementary Table 4).
218 Consistently with an ongoing pathogenic interaction, we found several defence related marker
219 genes among the differentially expressed genes (DEG). Members of the pathogenesis-related

220 (PR) family are prime markers of immune responses in several plant species, including
221 Marchantia (Carella et al., 2019, Gimenez-Ibanez et al., 2019) and we found that the expression
222 of several homologues showed opposite expression patterns when compared to mock treated
223 plants (Supplementary Table 5). Moreover, we observed that a conserved set of PTI markers,
224 shown to be activated in Marchantia upon interaction with bacteria (Gimenez-Ibanez et al.,
225 2019), oomycetes (Carella et al., 2019) and fungi (Redkar et al., 2022), were also induced in
226 response to TMV infection (Figure 3A). Additionally, a significant number of intracellular
227 receptors from the NLR family displayed upregulated expression upon TMV infection ($p < 6.245e-$
228 05 with those described by Bowman et al., (2017); $p < 1.308e-05$ with those described by Chia
229 et al., (2022); Supplementary Table 6). Nevertheless, none of them showed significant sequence
230 similarity to the NLR N gene triggering ETI responses in TMV infected tobacco plants (Whitham
231 et al., 1994). Likewise, several components from the RNA silencing machinery upregulated in
232 tobacco plants upon TMV infection (Sheng et al., 2019), were also differentially expressed in
233 response to TMV in Marchantia plants. The non-canonical *MpDCL1b (Mp6g09830)*, *MpDCL4*
234 *(Mp7g11720)*, and *MpRDR6 (Mp8g14970)* were upregulated, whereas *MpDCL3 (Mp1g02840)*,
235 *MpAGO9 (Mp8g08610)* and *MpNRPE1b (Mp6g00230)* were suppressed.

236 Gene Ontology (GO) analysis of the upregulated genes revealed an enrichment (padjust<0.05)
237 of biological processes related to reactive oxygen species, wounding, light intensity, heat
238 responses and responses to fungus and the presence of their constituent chitin (Supplementary
239 Table 7, Supplementary Figure 3A). Photosynthesis, DNA packaging and cell cycle, microtubule
240 organization or regulation of salicylic acid metabolism were among the downregulated processes
241 (padjust<0.05; Supplementary Table 8, Supplementary Figure 3B).

242 Notably, TMV is mainly transmitted through wounds and wounding response was one of the
243 upregulated processes in the GO analysis, which prompted us analysing this response. ERF
244 transcription factors are central to trigger wounding responses in vascular plants such as *A.*
245 *thaliana* (Heyman et al., 2018) with a conserved set of ERF transcription factors being also
246 recently described to respond to wounding in *Marchantia polymorpha* plants (Liang et al., 2022).
247 A subset of these wounding responsive ERF transcription factors showed the same expression
248 pattern upon TMV infection as that observed upon intensive wounding (Figure 3B, Liang et al.,
249 2022). To determine the whole transcriptional overlap between wounding and TMV responses,
250 we reanalysed published tissue incision transcriptomic responses (Liang et al., 2022) using the
251 same pipeline we used for the TMV samples. Comparison of both datasets showed a significant

252 overlap both in up-regulated (593 genes; p<6.631e-235) and down-regulated genes (162 genes;
253 p<2.137e-70; Figure 3C), suggesting that TMV infection contributes to a sustained wound
254 response in Marchantia.

255 Chitin is one of the most abundant polysaccharides in nature and it is a primary component of
256 cell walls in fungi and exoskeletons of arthropods such as insects, which in turn can work as viral
257 vectors in a range of plants species (Campbell, 1996). According to the GO enrichment in
258 response to chitin and fungi, and besides the fungal responsive genes described above as part
259 of a conserved PTI response, we also observed upregulation of a set of fungal responsive WRKY
260 transcription factors (Figure 3D; Redkar et al., 2022, Yotsui et al., 2023).

261 Photosynthetic deficiency is a hallmark for several stress responses, including those involving
262 viral infections. Accordingly, downregulation of transcripts involved in photosynthesis was one
263 of the main processes affected in our GO study as consequence of TMV infection. We determined
264 the photosynthetic efficiency in TMV infected areas from 10 Tak-1 plants after 2-weeks of
265 infection along with the very same area in mock treated plants. TMV infected areas showed a
266 significant reduction in photosynthetic competency when compared to similar areas from mock
267 treated plants (Figure 3E). Notably, parts of those very same plants distant to the infection foci,
268 showed also reduced photosynthetic capability, although to a lesser extent (Figure 3F). Those
269 results suggest that TMV responses might be systemic in *Marchantia polymorpha* plants.

270 As previously observed in *Nicotiana tabacum*, Marchantia plants infected with TMV are
271 compromised in cell cycle progression and DNA packaging (Jada et al., 2014). To further
272 corroborate the impact of TMV infection in the cell cycle, we infected Marchantia plants carrying
273 the G2-M reporter proMpCYCB;1:D-box-GUS (Hernandez-Garcia et al., 2021). TMV infected
274 plants showed reduced levels of the CYCB1 reporter as compared to mock treated plants (Figure
275 3G). That result supports the transcriptomic data pointing to reduced cell division upon TMV
276 infection.

277 Overall, those results show that TMV engages in a compatible interaction with *Marchantia*
278 *polymorpha*.

279 **Salicylic and OPDA-dependent signaling pathways are active at TMV infected areas**

280 The plant hormones Salicylic acid (SA) and Jasmonic acid (JA) are central in defence responses
281 against most pathogens of vascular plants, acting both in a synergistic and antagonistic manner.

282 Whereas the SA biosynthesis and signalling pathway are mostly conserved in *Marchantia*
283 *polymoprha* (Jia et al., 2023), the active molecules binding to the COI1 receptor and triggering
284 jasmonate signaling are a group of long chain polyunsaturated fatty acids, including dinor-OPDA,
285 instead of JA-Ile (Kneeshaw et al., 2022, Monte et al., 2018). Therefore, we compared the SA and
286 jasmonate-related transcriptomic responses with those found during TMV infection. To that end,
287 we used the time course datasets obtained on incubation of Marchantia with 1mM SA during 2,
288 6 and 12 hours (Jeon et al., 2022), SA concentration shown to promote defence against bacterial
289 and to increase susceptibility to fungal pathogens (Jeon et al., 2022, Matsui et al., 2020).
290 Comparison of the DEGs identified on SA treatment showed a significant overlap with those
291 responding to TMV infection (Figure 4A; Supplementary Figure 4). A total of 225 genes were
292 commonly up-regulated by 2 hours SA treatment or TMV ($p<1.799e-100$), 306 ($p < 1.382e-172$)
293 were shared after 6 hours treatment, and 92 ($p < 3.580e-47$) by 12 hours of SA incubation.
294 Likewise, TMV infection shared 47 down regulated genes ($p<1.618e-14$) with 2 hours, 38 ($p <$
295 $2.897e-13$) with the 6 hours, and 17 genes with 12 hours incubation samples ($p < 1.720e-05$),
296 showing that TMV infection activates SA-dependent transcriptional responses.

297 To ascertain a possible contribution from the jasmonate signalling pathway, we compared the
298 TMV transcriptional response with that of plants treated with dnr-OPDA (Monte et al., 2018) or
299 having a constitutively activated jasmonate pathway as a consequence of the mutation of the
300 JAZ1 signalling repressor (jaz1 KO plants; Monte et al., 2019). A total of 143 and 81 genes were
301 commonly up-regulated upon TMV infection and *jaz1* deficiency or dnr-OPDA treatment, while
302 238 were downregulated in TMV infected and jaz1 KO plants (Figure 4B)., suggesting that TMV
303 infection also activates the jasmonate signalling pathway in Marchantia.

304 To further understand which were the processes under control of SA and JA signalling pathways
305 on TMV infection, we carried out a GO analysis of the commonly regulated genes. This showed
306 that the JA pathway was responsible for activation in Marchantia of wounding, reactive oxygen
307 species and virus responses, in addition to the catabolism of several compounds, including lipids,
308 phenylpropanoids and salicylic acid. Interestingly, some of these processes were also
309 upregulated by SA treatment, including wounding, SA and lignin catabolism among others. The
310 SA response pathway was on the other side also responsible for the observed transcriptional up-
311 regulation of defence genes against bacteria and fungi, as well as responsive to chitin (Figure 4C,
312 Supplementary Table 9)

313 Furthermore, amongst the downregulated processes by JAZ1 deficiency and TMV infection were
314 translational elongation, mucilage and cell wall biosynthesis, response to fructose,
315 photosynthesis, microtubule-based process, growth, and response to abscisic acid (ABA; Figure
316 4D, Supplementary Table 9)

317 Collectively, those results show that SA and JA signalling pathways are activated in Marchantia
318 during TMV infection.

319 **TMV infection triggers aging in *Marchantia polymorpha***

320 Wound response, mitotic cell arrest, and reduced photosynthetic efficiency are hallmarks for
321 plant cell senescence (Espinoza et al., 2007, Gan, 2003). Senescence is the final stage of the life
322 cycle of a cell, tissue or organism and it is gradually triggered throughout aging. Additionally, SA
323 and JA, along with ET, contribute to senescence in *Arabidopsis thaliana* (Schommer et al., 2008,
324 Yu et al., 2021). Senescence can be also triggered by the interaction with different pathogens,
325 including the crucifer infecting TMV-Cg strain capable of compatible interactions with the
326 Arabidopsis UK-4 ecotype (Espinoza et al., 2007, Lim and Nam, 2005). Since all those senescence
327 hallmarks were present in our molecular characterization of the Marchantia-TMV interaction,
328 we first checked the expression levels of several senescence marker genes in our transcriptomic
329 data (Kulshrestha et al., 2022). We found that many of those senescence markers, such as
330 *MpMYB14* (Mp5g19050), *MpORE1* (Mp2g07720), *MpNYE1* (Mp1g17090) and *MpWRKY7*
331 (Mp3g17660), were induced upon TMV infection, hence suggesting that TMV infection could
332 trigger aging and tissue maturation in Marchantia. Transcriptional trajectories orchestrating
333 maturation and aging in Marchantia, both at organism and tissue level, have been recently
334 reported through transcriptional studies over developmental time or by analysing sections along
335 the thalli from top to base (Wang et al., 2023). Clustering the transcriptional profile of mock and
336 TMV infected plants with those datasets, based on Pearson's correlation coefficient and
337 regression model, showed that TMV infection promotes maturation and aging. Thus, while the
338 transcriptome from mock treated plants clustered with juvenile state samples (slide 2 and Day
339 1), that from TMV infected plants clustered with slide 4 and day 31 of development (Figure 5A,
340 5B).

341 Those results indicated that TMV infection triggers senescence in Marchantia, a characteristic
342 trait from compatible plant - virus interactions, and aging.

343 **MpNAC7 is a conserved interactor of the TMV silencing suppressor p126 and enhances defence**
344 **against TMV in tobacco plants.**

345 The TMV replicase p126 is essential for viral replication and movement, but it also works as a
346 silencing suppressor in vascular plants (Ding et al., 2004). To gain insights into its possible role
347 during TMV infection in Marchantia plants, we first established its subcellular location. We found
348 that p126 fused to GFP localized in cytoplasmatic bodies in mesophyll cells when transiently
349 expressed in *Nicotiana benthamiana* leaves (Figure 6A) consistently with earlier studies in onion
350 epidermal cells, where the full length p126 protein fused to GFP was found associated to the
351 endoplasmic reticulum (dos Reis Figueira et al., 2002). Similarly, Marchantia plants expressing
352 this very same construct, showed discrete cytoplasmic spot-like inclusions in oil body cells (Figure
353 6A), showing that p126 subcellular location is conserved between Nicotiana and Marchantia.

354 Constitutive expression of viral-derived silencing suppressors often leads to plant developmental
355 defects, like growth stunting (Kasschau et al., 2003). Accordingly, two-weeks old Marchantia
356 plants constitutively expressing p126 were smaller in size when compared to control plants
357 (Figure 6B).

358 The TMV replicase p126 is known to associate with several host factors in Arabidopsis, including
359 TOM1 (Yamanaka et al., 2000), GDI2 (Kramer et al., 2011) and the transcription factor ATAF2
360 (Wang et al., 2009). To assess whether those interactions were conserved between p126 and the
361 corresponding orthologs, we performed Y2H assays. Orthologs were identified by blasting the
362 Arabidopsis protein sequences at MarpolBase (https//Marchantia.info) and PlantRegMap
363 (http://plantregmap.gao-lab.org/). The P126 full length and helicase domain (nt 2442 to 3636)
364 were fused to the GAL4 binding domain and used as baits, while the putative interactors fused
365 to the GAL4-activation domain, were used as preys. Notably, the only conserved interaction was
366 that of the ortholog of the NAC transcription factor ATAF2, *MpNAC7* (Mp6g02620) (Figure 6C).
367 As for p126-ATAF2 binding (Wang et al., 2009), p126-MpNAC7 interaction could be confirmed *in*
368 *planta* using bimolecular luminescence complementation (Figure 6D). Moreover, interaction
369 with p126 was found to trigger proteasome dependent ATAF2 degradation in the context of TMV
370 infection (Wang et al., 2009), and in our assays luminescence signal from p126-MpNAC7
371 interaction was always lower when TMV was co-infiltrated together with MpNAC7 and p126. A
372 similar reduction was not observed in the presence of TuMV, indicating that specific MpNAC7
373 degradation during TMV infection is a conserved feature in Marchantia (Figure 6D).

374 In Arabidopsis, ATAF2 expression is triggered by TMV infection (Wang et al., 2009). Likewise, we
375 found that MpNAC7 expression is also increased on TMV infection (Log2(fold-change)= 0.991),
376 wounding (Log2(fold-change)= 2.67), dnr-OPDA and after 6 hours of SA treatment (Log2(fold-
377 change)= 1,23) in Marchantia. Likewise, ATAF2 is induced by wounding, SA and JA treatments
378 (Delessert et al., 2005) and contributes to defence against TMV in Arabidopsis (Wang et al.,
379 2009). Here, to ascertain the role of MpNAC7 in defence against TMV, and rule out a possible
380 connection with RNA silencing- mediated responses, we infected 1 month old Nicotiana plants
381 deficient in RDR6 (rdr6i; (Schwach et al., 2005)) with MpNAC7, or GUS as control, in the presence
382 of TMV or TuMV. TMV and TuMV strains were labelled with the ROS1 gene which triggers
383 anthocyanin production, and hence we followed presence of the viruses by the purple colour
384 (Bedoya et al., 2012). We observed that co-expression of MpNAC7 abrogated local and systemic
385 TMV infection with respect to plants co-expressing the GUS control. By contrast, MpNAC7 co-
386 expression was of no effect on TuMV infected plants, that displayed a similar local and systemic
387 presence of the virus as the GUS co-infiltrated controls (Figure 6E, Supplementary Figure 5).

388 Collectively, those results show that molecular interaction between the TMV silencing
389 suppressor p126 and the host NAC transcription factor is conserved in Marchantia, as well as the
390 role of this transcription factor in defence.

391 **Discussion**

392 In this work, we have characterized the interaction of the non-vascular liverwort *Marchantia*
393 *polymoprha* with viruses. First, we have defined known and unknown viruses that associate with
394 Marchantia in natural settings. These studies show that Marchantia is primarily associated with
395 RNA viruses in nature, validating previous predictions based on the presence of viral gene
396 hallmarks in the transcriptomes from the 1000 Plants Genome Project (Mushegian et al., 2016).
397 We also showed that at least one of these newly discovered viruses is able to replicate in
398 laboratory grown Marchantia Tak-1 plants. Second, we have found that TMV engages into a
399 compatible interaction with Marchantia plants. That interaction encompasses an extensive
400 transcriptional reprogramming reminiscent of that found in vascular plants such as Arabidopsis
401 and Nicotiana, albeit involving also previously uncovered differences like the activation of a
402 sustained wounding response. Third, we have found that the TMV silencing suppressor p126
403 displays similar subcellular location in Marchantia cells, as in Nicotiana, and that its interaction
404 with a NAC transcription factor, MpNAC7, also specifically abrogates TMV infection in Nicotiana

405 plants. All those commonalities show that core molecular events of plant-virus interactions
406 found in vascular plants are also present in non-vascular plants.

407 Marchantia plants infected with TMV undergo a transcriptional reprogramming consistent with
408 a pathogenic process and characterized by the activation of the defence related PR proteins and
409 a conserved PTI response. Perception of dsRNAs have been found to trigger PTI in response to
410 TMV infection in Arabidopsis, which in turn contributes to antiviral defence (Korner et al., 2013).
411 Indeed, dsRNA-triggered PTI is dependent on the Arabidopsis PRR co-receptor SERK1 (Niehl et
412 al., 2016), which has a corresponding ortholog in the Marchantia genome (Mp7g09160), and
413 which was shown to be involved in PTI against *Pseudomonas syringae,* and to be targeted by the
414 PTI suppressors AvrPto (Gimenez-Ibanez et al., 2019). Thus, it will be interesting in future studies
415 to analyse the role of MpSERK1 in viral PTI responses. Additionally, TMV infection triggers the
416 expression of a significant number of NLR genes that can potentially contribute to an ETI
417 response. In the absence of a DCL2 gene in Marchantia, we also observed changes on the
418 expression of core genes of the RNA silencing machinery in response to TMV infection. In
419 contrast to the repression of elements from the RNA-Directed DNA methylation pathway, such
420 as *MpDCL3*, *MpAGO9* and *MpNRPE1b*, the central elements within the RNA antiviral machinery
421 *MpDCL4* and *MpRDR6* were activated. Such general switch on RNA silencing pathways in
422 Marchantia is reminiscent of that found specifically restricted to the vasculature of *Nicotiana*
423 *benthamiana* in response to TMV (Collum and Culver, 2017). Those results suggest an
424 evolutionary re-routing of defence mechanisms after acquisition of novel tissues or cell-types
425 that become new focal points for plant-virus interactions.

426 Interestingly, our results also uncover a previously unknown potential role of wound response
427 as an antiviral defence mechanism. Plant cells undergoing wound responses experience
428 inhibition of their photosynthetic ability becoming sink tissues on the transport of
429 photoassimilates (Quilliam et al., 2006), attracting TMV movement (Brants, 1961). Thus, it is
430 tempting to speculate that sustained wound response in Marchantia plants, along with local and
431 systemic decreased on photosynthetic capability and senescence confine TMV infection
432 preventing its movement throughout the plant.

433 Additionally, salicylic and jasmonate pathways are central for defence against several pathogens.
434 A spatially complementary synergistic interaction of both was observed to be necessary for
435 defence against *Pseudomonas syringae* in Arabidopsis (Betsuyaku et al., 2018, Salguero-Linares
436 et al., 2022). Likewise, their synergistic interaction is responsible for local and systemic resistance

437 against TMV in *Nicotiana benthamiana* (Zhu et al., 2014). In line with what was found in
438 Nicotiana, our results show that both pathways are activated in Marchantia plants upon TMV
439 infection, whilst initial results, show that both pathways are antagonistically involved in
440 Marchantia in the defence against fungal and bacterial pathogens (Gimenez-Ibanez et al., 2019,
441 Matsui et al., 2020).

442 Our work also highlights the conservation of central players, such as MpNAC7, in the specific
443 defence against TMV. Future research might focus on comparative studies to ascertain the
444 conservation of the genetic networks under MpNAC7 and ATAF2 regulation both in Marchantia
445 and Arabidopsis.

446 Collectively, results from this work suggest the presence of evolutionary conserved and divergent
447 plant strategies to cope with viral infections. Those might include gain and loss of defence
448 strategies, such as those involving wound responses. Evolution of plant-virus interactions might
449 also encompass the gradual acquisition of new elements within the underlying gene networks,
450 as those physically interacting with pathogen-derived proteins. Finally, defence mechanisms
451 might undergo re-location to newly pathogen-targeted cell-types and tissues over evolutionary
452 times.

453

454 **Material and methods**

455 *Plant growth conditions*

456 Male *Marchantia polymorpha* plants Takaragaike-1 (Tak-1) were grown on plates with half
457 strength Gamborg´s B5 medium (Duchefa) containing 1% agar and 1% sucrose under continuous
458 light and 22ºC.

459 *Nicotiana benthamiana* plants were grown on soil under long day conditions (16h light/ 8h dark)
460 and 25ºC.

461 *Infection assays*

462 Frozen tissue from Marchantia plants from the Tübingen population or lab grown Tak-1 plants
463 was homogenized in liquid nitrogen cold mortars, resuspended in phosphate buffer pH7.2,
464 filtered using 70 µM filters and kept at 4ºC. Two-week old Tak-1 plants grown in sterile conditions
465 in plates were vacuum incubated with each of both extracts and transferred to plates containing

466 wet soil. Eight Tak-1 individuals exposed to each sap were collected either one or two weeks
467 after incubation to assess viral replication.

468 Two weeks-old *Nicotiana benthamiana* plants were infiltrated with an agrobacterium solution
469 (0.5 O.D) carrying the TMV-GFP clone (Peart et al., 2002). Infected Nicotiana plants were grown
470 for 3 additional weeks along with non-infected plants and upper leaves displaying infection
471 symptoms were collected, along with equivalent ones from non-infected plants and frozen in
472 liquid nitrogen. Subsequently, leaf tissue was grinded in a liquid nitrogen cold mortar. Sap was
473 isolated from grinded leaf tissue using phosphate buffer pH 7.2, filtered with 70 µM filters and
474 maintained at 4ºC. Two-weeks old Tak-1 plants were incubated either in TMV-GFP containing sap
475 or sap from non-infected plants (mock) for 5 minutes in vacuum. After incubation, Tak-1 plants
476 were transferred to plates containing wet soil and brought back to the growth chamber. GFP
477 signal was monitored 1 and 2 weeks after incubation using a portable UV lamp or with a
478 magnifying stereoscope couple to a UV light source.

479 *RNA isolation and expression analysis*

480 Total RNA was extracted from Marchantia plants using the protocol described in Box et al.,
481 (2011). Isolated RNA was further cleaned using the RNeasy Kit (Qiagen). 500 ngs of total RNA
482 were DNase I treated (Fisher Scientific) and converted into cDNA using the RevertAid first strand
483 kit (Fisher Scientific) following the manufacturer instructions. RT-qPCR experiments were
484 performed in a lightcycler (ROCHE) device. Relative expression changes were calculated using
485 the $2^{-\Delta\Delta Ct}$ method using *MpACTIN7* (Mp6g11010) gene as housekeeping. Primers utilized can be
486 found in supplementary table 8.

487 *RNA-seq analysis*

488 For virome studies, 1 µg of total RNA from each of the 14 individuals included in the study was
489 pooled and 4 µg from the mixture were used for preparing a single library using total ribo-
490 depleted RNA following the manufacturer instructions (Illumina TruSeq Stranded total RNA LT
491 sample prep Kit, plant) and sequenced on a Illumina NovaSeq 6000 device in 2x150 bp mode. A
492 total of 306,895,552 reads were obtained. The reads were trimmed and further analysed using
493 QIAGEN CLC Genomics Workbench 21 (https://digitalinsights.qiagen.com/). Dataset was
494 analysed for the presence of known and new viruses using an established virus detection
495 pipeline (Pecman et al., 2017), which includes: reads trimming, *de novo* assembly of trimmed
496 reads, mapping of reads and contigs to NCBI viral RefSeq database (search for known viruses)

497 and pFam domain search for contig sequences (search for known and unknown viruses). To
498 detect known viruses, results of reads mapping to viral RefSeq database were inspected and
499 filtered for viruses for which at least 1000 nts of the reference sequence were covered by
500 mapped reads (Supplementary table 1). In parallel, to detect known viruses and search for new
501 ones, results of the pFam domain search of contig sequences were filtered for hits to viral
502 proteins. Then, this candidate list of viral contigs was additionally queried for similarity against
503 complete NCBI *nr* database (October 2020) using blastx (Gish and States, 1993) and the similarity
504 search results were visualized and taxonomically classified using MEGAN 6 (Huson et al., 2016).
505 Contigs corresponding to cellular organisms in this analysis were excluded from the list to obtain
506 a final list of putative viral-like sequences (Supplementary table 2). Trimmed sequencing reads
507 were mapped to the list of putative viral-like sequences, to estimate the abundance of
508 corresponding nucleic acids in the sequenced sample and the results were reported as average
509 mapping depth (number of times a position is covered by sequencing reads, averaged over a
510 complete contig length; Supplementary table 2).

511 For a newly discovered picorna-like virus, named Tübingen picorna-like virus 1, additional
512 analyses were performed, aiming to ascertain its association with *M. polymorpha*. Amino acid
513 sequence of ORF 1 of the virus (containing RNA-dependent polymerase (RdRp) domain) was
514 queried for similarity against complete NCBI *nr* database (January 2022) using blastp. Fifteen
515 best hits according to bit score values (which have at least 33% identity with the conserved part
516 of the RdRp domain of the queried virus) were included into phylogenetic analysis. Alignment of
517 the sequences of the conserved part of RdRp was performed using MAFFT 7.48 (Katoh and
518 Standley, 2013), followed by alignment trimming using TrimAI 1.3 in Automated 1 mode (Capella-
519 Gutiérrez et al., 2009). Then, best protein substitution model was selected using Model Finder
520 (Kalyaanamoorthy et al., 2017) and maximum likelihood phylogenetic tree inference was
521 performed based on the trimmed alignment using IQ-Tree 1.6.12 (Nguyen et al., 2015), using
522 1000 ultrafast bootstrap replicates (Hoang et al., 2018). The resulting phylogenetic tree was
523 visualized using iTOL 6.5 (Letunic and Bork, 2021) and viral taxa on the tree were coloured
524 according to the associated sample source, as designated in NCBI GenBank.

525 For analysing the transcriptional response in Marchantia plants to TMV infection, 1 ug of total
526 RNA was used for preparing each stranded library by mRNA enrichment following manufacturer
527 indications (TrueSeq kit from Illumina). Libraries were sequenced on a Novaseq 6000 device. A
528 total of 20-21 million pairs were obtained per sample. Adapter removal and trimming of low

529 quality bases was done using Trim Galore! v0.6.1
530 (https://www.bioinformatics.babraham.ac.uk/projects/trim_galore/), removing reads shorter
531 than 20 bps and non-paired reads after the trimming step. Ribosomal RNA reads were removed
532 using SortMeRNA v2.1b (Kopylova et al., 2012), removing also reads that become unpaired after
533 this filtering step.

534 Cleaned reads together with the transcriptome of *Marchantia polymorpha* were used to quantify
535 gene expression at transcript level using Salmon v1.1.0 (Patro et al., 2017).

536 For this, the file MpTak1v5.1_r1.mrna.fasta containing the Marchantia transcriptome (v5.1) was
537 downloaded from https://marchantia.info/download/tak1v5.1/ (as of 19-Jan-2021). This file was
538 indexed using *Salmon index* and then used as input for *Salmon quant*, which was ran with
539 parameters -l A, –validateMappings, --recoverOrphans, --rangeFactorizationBins 4, --seqBias,
540 and –gcBias. Mapping rate was found to be in the 89.5%-92.58% range.

541 The R progam tximport v1.14.2 (Soneson et al., 2015) was used to aggregate Salmon's transcript
542 expression estimates at gene level and the *DESeqDataSetFromTximport* from the R package
543 DESeq2 v1.26.0 (Love et al., 2014) was used to create an R object with count data and
544 experimental information for all samples. A low-expression filter was then applied to remove any
545 gene with less than 10 counts across all 8 analyzed samples, resulting in a final set of 14,980
546 genes (from 19,217 annotated genes). Then, the *DESeq* function, which, among other things,
547 computes size factors for sample normalization, was applied to the filtered object. DESeq2's *rlog*
548 function was used to transform count data to the log2 scale while minimizing for differences
549 between samples for low-expressed genes. The transformed data was fed to DESeq2's *plotPCA*
550 function to visualize a PCA plot of the samples.

551 The analysis of differential expression was done using DESeq2's *results* function with the filtered
552 and normalized object as input and parameter *alpha = 0.05.*

553 All datasets used in this study for comparative analysis (wound response and salicylic acid time
554 course) were analysed in the very same way as described above.

555 All Gene ontology analysis (GO) were performed using PLAZA
556 (https://bioinformatics.psb.ugent.be/plaza/). Redundancy on representative categories was
557 reduced using Revigo (http://revigo.irb.hr/).

558 For correlation analysis of transcriptome responses between developmental trajectories and
559 TMV response, raw reads were processed as described above, except that rRNA was removed
560 using ribodetector_cpu v0.2.7 (Deng et al., 2022) and Salmon version was v1.9.0. Salmon's
561 counts were converted into a DESeq2 object and a low-expression filter was applied as described
562 above. Next, the existing batch effect between time course samples and sliced tissue ones was
563 removed using the Combat_seq function from the sva package (Leek et al., 2023), v3.48.0. Then,
564 values for biological replicates were averaged and Pearson correlation was computed for the
565 resulting count matrix and displayed using the Heatmap function from the ComplexHeatmap
566 package (Gu, 2022). The batch correction, correlation and heatmap plotting steps were based
567 on the R script used in (Wang et al., 2023) and kindly provided by the authors.

568 *Constructs and plant transformation*

569 cDNA from Marchantia mock treated plants was used to amplify the coding regions of *MpTOM1*
570 (Mp3g00660), *MpGDI2* (Mp6g05010) and *MpNAC7* (Mp6g02620) by PCR using Phusion
571 polymerase (NEB). Arabidopsis *Bobber1* (At5g53400) was amplified using cDNA synthesized from
572 RNA from Arabidopsis infolorescences. DNA was isolated from four-weeks old plants using
573 extraction buffer (200mM Tris pH 7.5, 25 mM EDTA, 250 mM Na Cl, 0.5% SDS) followed by
574 isopropanol precipitation, washed with Ethanol 70%, and resuspended in MiliQ sterile water.
575 Isolated DNA was used as template to amplify the genomic region covering the promoter and
576 degron to generate the MpCYCD1;1B:GUS reporter by amplification in 5 overlapping fragments
577 that were included in a final PCR to reconstruct the final region. P126 was amplified using DNA
578 from the TMV-GFP containing plasmid. All obtained fragments were further incubated with dATP
579 and Taq DNA polymerase (NEB) for 1 hour before cloned into the gateway compatible vector
580 PCR8/GW/TOPO TA (Invitrogen). An entry vector containing the Arabidopsis AGO1 was kindly
581 provided by Pablo Manavella. Inserts were cloned into their final vectors through LR reaction
582 using LR clonase II (Invitrogen). All plasmids were submitted to Sanger sequencing to corroborate
583 their integrity before used in the corresponding experiments. A list of used primers and
584 constructs can be found in supplementary table 10 and supplementary table 11.

585 Plant transformation was performed as described in Ishizaki et al., (2008)and selected in
586 Gamborg´s B5 media supplemented with Kanamycin 100mg/ml and Cefotaxime 100mg/ml.

587 *Histology and imaging*

588 Marchantia plants were embedded in 3% agarose and cross-sections of around 200 µM were
589 obtained using a vibratome. A total of 12 MpCYCD1;1B:GUS reporter plants, either TMV infected
590 or mock, were fixed in 90 % acetone, and GUS activity was assayed as described in Blazquez et
591 al., (1997). Confocal imaging was performed using Leica SP5. Images were processed using Fiji
592 (Schindelin et al., 2012).

593 *Protein-protein interaction assays*

594 Interactions in the yeast two-hybrid system was assayed on selective medium (L^-, W^-, H^-). The
595 assay was repeated 3 times. For the luciferase complementation assay, one-month old rdr6i
596 Nicotiana plants were used. *Agrobacterium tumefaciens* cultures with the different constructs
597 were mixed in the same amounts at a final OD_{600}=0.6. Leaves were imaged three days after
598 inoculation using a LAS4000 device.

599 *Photosynthetic measurements*

600 10 infected and 10 mock treated plants were subjected to 10 measures each using a IMAGING-
601 PAM Maxi device (Heinz Walz GmbH). Quantification was done using the ImagingWing integrated
602 software.

603 **Acknowledgments**

604 We would like to Juan Jose López-Moya, Miguel A. Blázquez and Salomé Prat for critical reading
605 of the manuscript. Sebastian Schornack, Phil Carella, Alexander Summers, the CUBG curation
606 team (Samuel Brockington and Mar Millan), Klaus Schlaeppi, Katja Rembold, Alba Gonzalez,
607 Detlef Weigel, Alexandra Kehl and Brigitte Fiebig for their help in obtaining Marchantia
608 individuals for the virome assays. We would like to thank Eduardo Bejarano for providing the
609 plasmid containing TMV-GFP and Antonio Darós for providing TuMV-ROS1 and TMV-ROS1
610 containing plasmids. Pablo Manavella for the AtAGO1-pEntr plasmid. Phil Carella for an updated
611 annotation of NLR genes in Marchantia. We would also thank to Jia-Wei Wang, Long Wang and
612 Jie Xu for sharing the code used for correlation analysis between TMV transcriptional responses
613 and the different samples from Marchantia developmental trajectories.

614 The work in the MoRE lab is funded by RYC-2015-19154 (funded by MCIN/AEI/
615 10.13039/501100011033 and by "ESF Investing in your future"), RTI2018-097262-B-I00 (funded
616 by MCIN/AEI/ 10.13039/501100011033 and by "ERDF A way of making Europe") and through
617 the "Severo Ochoa Programme for Centres of Excellence in R&D" 2016-2019 (SEV-2015-0533)

618 and 2020-2023 (CEX2019-000902-S) funded by MCIN/AEI/ 10.13039/501100011033 and the
619 CERCA programme from the Generalitat de Catalunya to I-R-S. T J-G was recipient of a
620 Postdoctoral Fellowship from CRAG through the "Severo Ochoa Programme for Centres of
621 Excellence in R&D" 2016-2019 (SEV-2015- 0533). L. V-M was supported by BES-2016-076986
622 (funded by MCIN/AEI/ 10.13039/501100011033 and by "ESF Investing in your future"). The work
623 at NIB was funded by Slovenian Research and Innovation Agency core and project financing P4-
624 0407, P4-0165 and J4-4553.

625 Data access: Raw data from the virome has been deposited in SRA and GenBank under Bioproject
626 (PRJNA1022866) and BioSample (SAMN37631837). Raw data from TMV infected vs. Mock
627 treated plants have been deposit GEO (GSE241827). Reconstructed genomic sequences of three
628 novel viruses uncovered by virome analysis were deposited in NCBI GenBank (OR640980-82).

629 **Figure legends**

630 **Figure 1.** *Marchantia polymorpha is infected by RNA viruses.*

631 (A) Genome structure of Tübingen picorna-like virus 1, newly discovered in composite *M.*
632 *polymorpha* sample with two predicted open reading frames (ORFs) and corresponding
633 average reads mapping depth in sequenced composite sample.

634 (B) Maximum likelihood phylogenetic tree obtained based on the alignment of the
635 conserved part of RdRd of Tübingen picorna-like virus 1 and fifteen other most similar
636 viruses. The tree was midpoint rooted. Coloured virus names correspond to the sources
637 associated with a particular virus, according to the legend on the right side of the panel.
638 Numbers next to the branches represent statistical support (%) of the clades according to
639 the ultrafast bootstrap analysis. Codes next to the taxon names in round brackets are the
640 corresponding NCBI GenBank protein accession numbers. Next to them, fractions in square
641 brackets represent % of identity of Tübingen picorna-like virus 1 to other individual taxons
642 for the aligned part of the RdRp domain.

643 (C) Results of the viral concentration measurements for *M. polmorpha* plants inoculated
644 with Tübingen picorna-like virus 1 positive plant extracts. On the right, relative
645 concentrations of Tübingen picorna-like virus 1 in inoculated plants one- and two-weeks
646 post inoculation are shown; measurements of concentrations in individual plants are shown
647 as dots and the box-whisker plots represent the distribution of values for the two time

648 points (at 1 WPI, x represent an outlier measurement). On the top of the plot, the horizontal
649 connecting line designates statistically significant difference in the means of the two
650 distributions, with the corresponding p-value, according to the nonparametric Wilcoxon
651 rank sum test.

652 **Figure 2**. *Tobacco mosaic virus replicates in Marchantia plants*.

653 (A) GFP fluorescent signal increases in plants after 1 week, (left panel) compared to 2-weeks
654 infected plants (right panel). Both images show the same part or an infected plant under
655 a magnification device under UV light. Red shows chlorophyll autofluorescence. White
656 bar scale shows 100 µms.
657 (B) TMV-GFP transcripts increase over time in infected plants. Pools of three plants were
658 used for each time point. T0 corresponds to samples collected immediately after sap
659 incubation, while T1 and T2 correspond to samples collected 1 and 2 weeks after
660 incubation.
661 (C) TMV-GFP infects all cell types. Transversal section of and infected area under confocal
662 image. The picture shows the merge between green (virus) and red (autofluorescence)
663 channels. Merge was performed using Fiji. P stands for Photosynthetic region, S for
664 storage region and E stands for lower epidermis. White bar scale shows 1 µm.

665 **Figure 3.** *TMV triggers stress-related molecular reprogramming in Marchantia.*

666 (A) Set of wound responsive ERF transcription factors.
667 (B) Venn diagram showing that transcriptional reprogramming upon TMV infection largely
668 overlaps with that found upon wounding.
669 (C) Set of chitin and TMV responsive WRKY transcription factors in Marchantia.
670 (D) Set of common PTI marker genes responsive to fungi, bacteria and TMV.
671 (E) Photosynthetic efficiency (Fv/Fm) in infected areas compared to equivalent areas from
672 mock treated plants. Statistical assessment was performed using a parametric T-test.
673 (F) Photosynthetic efficiency (Fv/Fm) in non-infected areas, from infected plants, compared
674 to equivalent areas from mock treated plants. Statistical assessment was performed
675 using a parametric T-test.
676 (G) TMV infected plants show lower cell cycle activity as inferred from MpCYCD1;1B:GUS
677 reporter. Left, staining from reporter plants incubated in sap from mock plants. Right,
678 staining from reporter plants infected with TMV.

679 **Figure 4**. *Salicylic and jasmonate signalling pathways are activated during Marchantia-TMV*
680 *interaction.*

681 (A) Venn diagrams showing the overlap between the transcriptional responses under TMV
682 infection ad a salicylic treatment time course (2 and 6 hours).
683 (B) Overlap between the trancriptome responses to TMV and jaz1ko mutants with
684 constitutively active jasmonate signalling, left, and treatment with the active dnr-OPDA
685 jasmonate.
686 (C) Biological processes commonly upregulated in response to TMV infection, SA treatment
687 (2,6 and 12h) and activation of jasmonate signalling.
688 (D) Biological processes commonly downregulated in response to TMV infection, SA
689 treatment (12h) and activation of jasmonate signalling.

690 **Figure 5.** *TMV infection triggers maturation and aging in Marchantia*.

691 (A) Pairwise comparison between mock and TMV samples along with sliced thallus samples.
692 (B) Pairwise comparison between mock and TMV samples along with samples from
693 Marchantia developmental series (D, states the days after gemma germination
694 Marchantia samples were collected)

695 **Figure 6.** *Conservation of the interaction between Marchantia and the TMV silencing suppressor*
696 *p126.*

697 (A) P126-GFP shows accumulation in cytoplasmic bodies both in *Nicotiana benthamiana*
698 and *Marchantia polymorpha* under confocal microscopy. Scale bar is 100 µMs.
699 (B) Overexpression of p126 inhibits growth (area) when compared to Tak-1 control plants.
700 Analysis was done on 6 individual plants per genotype and using a two tailed-t-test.
701 (C) MpNAC7 interacts with the helicase domain of p126 in yeast.
702 (D) MpNAC7 interacts both with the helicase and the full length p126 in planta.
703 (E) Transient expression of MpNAC7 in Nicotiana plants abrogates local and systemic TMV
704 infection. TMV presence is shown as purple.

705 **Supplementary figure 1**. *Nicotiana benthamiana plants inoculated with sap from Marchantia*
706 *infection experiments.*

707 (A) Nicotiana plants inoculated with sap from mock treated plants. Upper panel, top view
708 of plant with white light. Down panel, same Nicotiana plant under UV light.

709 (B) Nicotiana plants inoculated with sap from TMV-GFP treated plants. Upper panel, top
710 view of plant with white light showing crinkled and yellowish leaves as result of TMV
711 infection. Down panel, same Nicotiana plant under UV light showing GFP signal from
712 TMV infection in leaves showing symptoms.
713 (C) Inset from a TMV-GFP infected leaf showing symptoms of infection (reduced chlorophyll
714 content) in the upper panel, coinciding with TMV-derived GFP signal under UV light.

715 **Supplementary figure 2**. *Sampling and validation of samples for transcriptomic assays.*

716 (A) Example of areas collected from mock, upper panel, and TMV-GFP infected plants for
717 transcriptomic assays.
718 (B) RT-qPCR validation of TMV-GFP levels in the 4 pools used for RNA-seq.
719 (C) Principal component analysis of the different replicates from RNA-seq experiment.

720 **Supplementary figure 3.** *Gene ontology analysis of biological processes to which DEGs in respond*
721 *to TMV infection belong.*

722 (A) GO categories from upregulated genes in response to TMV infection.
723 (B) Selected GO categories from downregulated genes in response to TMV infection.

724 **Supplementary figure 4.** *Overlap between DEGs responding to 12 hours of incubation in salicylic*
725 *acid and those responsive TMV infection.*

726 **Supplementary figure 5.** *MpNAC7 specifically abrogates TMV infection in Nicotiana plants.*

727 (A) Picture of inoculated leaves showing that MpNAC7 abrogates local TMV but not TuMV
728 infection (purple colour).
729 (B) Effect in systemic leaves.
730 (C) Upper view of infected plants.

731 **Supplementary table 1.** *Detection of viral sequences of known viruses*.

732 **Supplementary table 2.** *Detection of known and putative novel virus-like sequences*.

733 **Supplementary table 3.** *Demographic study for the presence of a set of known and newly*
734 *identified virus in individuals from the different sampling sites*.

735 **Supplementary table 4.** *List of DEG in response to TMV infection in Marchantia.*

736 **Supplementary table 5.** *List of Pathogenesis-related (PR) genes differentially expressed upon*
737 *TMV infection.*

738 **Supplementary table 6.** *List of NLR genes differentially expressed upon TMV infection*

739 **Supplementary table 7.** *List of GO categories of the upregulated biological processes in response*
740 *to TMV infection.*

741 **Supplementary table 8.** *List of GO categories of the downregulated biological processes in*
742 *response to TMV infection.*

743 **Supplementary table 9.** *List of GO categories of the biological processes commonly responsive*
744 *to TMV infection and salicylic acid time course treatment, jaz1ko mutants and dnr-OPDA*
745 *treatment.*

746 **Supplementary table 10.** *Table of construct used in this study.*

747 **Supplementary table 11.** *Table of primers used in this study.*

748

749 **Bibliography:**

750 BALLY, J., NAKASUGI, K., JIA, F., JUNG, H., HO, S. Y., WONG, M., PAUL, C. M., NAIM, F., WOOD, C.
751 C., CROWHURST, R. N., HELLENS, R. P., DALE, J. L. & WATERHOUSE, P. M. 2015. The
752 extremophile Nicotiana benthamiana has traded viral defence for early vigour. *Nat*
753 *Plants,* 1**,** 15165.
754 BECK, M., WYRSCH, I., STRUTT, J., WIMALASEKERA, R., WEBB, A., BOLLER, T. & ROBATZEK, S. 2014.
755 Expression patterns of flagellin sensing 2 map to bacterial entry sites in plant shoots and
756 roots. *J Exp Bot,* 65**,** 6487-98.
757 BEDOYA, L. C., MARTINEZ, F., ORZAEZ, D. & DAROS, J. A. 2012. Visual tracking of plant virus
758 infection and movement using a reporter MYB transcription factor that activates
759 anthocyanin biosynthesis. *Plant Physiol,* 158**,** 1130-8.
760 BETSUYAKU, S., KATOU, S., TAKEBAYASHI, Y., SAKAKIBARA, H., NOMURA, N. & FUKUDA, H. 2018.
761 Salicylic Acid and Jasmonic Acid Pathways are Activated in Spatially Different Domains
762 Around the Infection Site During Effector-Triggered Immunity in Arabidopsis thaliana.
763 *Plant Cell Physiol,* 59**,** 439.
764 BLAZQUEZ, M. A., SOOWAL, L. N., LEE, I. & WEIGEL, D. 1997. LEAFY expression and flower
765 initiation in Arabidopsis. *Development,* 124**,** 3835-44.
766 BOWLES, A. M. C., PAPS, J. & BECHTOLD, U. 2022. Water-related innovations in land plants
767 evolved by different patterns of gene cooption and novelty. *New Phytol,* 235**,** 732-742.
768 BOWMAN, J. L., KOHCHI, T., YAMATO, K. T., JENKINS, J., SHU, S., ISHIZAKI, K., YAMAOKA, S.,
769 NISHIHAMA, R., NAKAMURA, Y., BERGER, F., ADAM, C., AKI, S. S., ALTHOFF, F., ARAKI, T.,
770 ARTEAGA-VAZQUEZ, M. A., BALASUBRMANIAN, S., BARRY, K., BAUER, D., BOEHM, C. R.,
771 BRIGINSHAW, L., CABALLERO-PEREZ, J., CATARINO, B., CHEN, F., CHIYODA, S., CHOVATIA,
772 M., DAVIES, K. M., DELMANS, M., DEMURA, T., DIERSCHKE, T., DOLAN, L., DORANTES-

773 ACOSTA, A. E., EKLUND, D. M., FLORENT, S. N., FLORES-SANDOVAL, E., FUJIYAMA, A.,
774 FUKUZAWA, H., GALIK, B., GRIMANELLI, D., GRIMWOOD, J., GROSSNIKLAUS, U.,
775 HAMADA, T., HASELOFF, J., HETHERINGTON, A. J., HIGO, A., HIRAKAWA, Y., HUNDLEY, H.
776 N., IKEDA, Y., INOUE, K., INOUE, S. I., ISHIDA, S., JIA, Q., KAKITA, M., KANAZAWA, T.,
777 KAWAI, Y., KAWASHIMA, T., KENNEDY, M., KINOSE, K., KINOSHITA, T., KOHARA, Y., KOIDE,
778 E., KOMATSU, K., KOPISCHKE, S., KUBO, M., KYOZUKA, J., LAGERCRANTZ, U., LIN, S. S.,
779 LINDQUIST, E., LIPZEN, A. M., LU, C. W., DE LUNA, E., MARTIENSSEN, R. A., MINAMINO,
780 N., MIZUTANI, M., MIZUTANI, M., MOCHIZUKI, N., MONTE, I., MOSHER, R., NAGASAKI,
781 H., NAKAGAMI, H., NARAMOTO, S., NISHITANI, K., OHTANI, M., OKAMOTO, T.,
782 OKUMURA, M., PHILLIPS, J., POLLAK, B., REINDERS, A., ROVEKAMP, M., SANO, R., SAWA,
783 S., SCHMID, M. W., SHIRAKAWA, M., SOLANO, R., SPUNDE, A., SUETSUGU, N., SUGANO,
784 S., SUGIYAMA, A., SUN, R., SUZUKI, Y., TAKENAKA, M., et al. 2017. Insights into Land Plant
785 Evolution Garnered from the Marchantia polymorpha Genome. *Cell,* 171**,** 287-304 e15.
786 BOX, M. S., COUSTHAM, V., DEAN, C. & MYLNE, J. S. 2011. Protocol: A simple phenol-based
787 method for 96-well extraction of high quality RNA from Arabidopsis. *Plant Methods,* 7**,**
788 7.
789 BRANTS, D. H. 1961. The Influence of Meristematic Tissue and Injuries on the Transport of
790 Tobacco Mosaic Virus in Nicotiana tabacum L. cultivar. Samsun. *Acta Botanica*
791 *Neerlandica,* 10**,** 113-163.
792 CAMPBELL, R. N. 1996. Fungal transmission of plant viruses. *Annu Rev Phytopathol,* 34**,** 87-108.
793 CAPELLA-GUTIÉRREZ, S., SILLA-MARTÍNEZ, J. M. & GABALDÓN, T. 2009. trimAl: a tool for
794 automated alignment trimming in large-scale phylogenetic analyses. *Bioinformatics,* 25**,**
795 1972-1973.
796 CARELLA, P., GOGLEVA, A., HOEY, D. J., BRIDGEN, A. J., STOLZE, S. C., NAKAGAMI, H. &
797 SCHORNACK, S. 2019. Conserved Biochemical Defenses Underpin Host Responses to
798 Oomycete Infection in an Early-Divergent Land Plant Lineage. *Curr Biol,* 29**,** 2282-2294
799 e5.
800 CARELLA, P., GOGLEVA, A., TOMASELLI, M., ALFS, C. & SCHORNACK, S. 2018. Phytophthora
801 palmivora establishes tissue-specific intracellular infection structures in the earliest
802 divergent land plant lineage. *Proc Natl Acad Sci U S A,* 115**,** E3846-E3855.
803 CHIA, K.-S., KOURELIS, J., VICKERS, M., SAKA, I. T., KAMOUN, S. & CARELLA, P. 2022. The N-
804 terminal executioner domains of NLR immune receptors are functionally conserved
805 across major plant lineages. *bioRxiv*.
806 COLLUM, T. D. & CULVER, J. N. 2017. Tobacco mosaic virus infection disproportionately impacts
807 phloem associated translatomes in Arabidopsis thaliana and Nicotiana benthamiana.
808 *Virology,* 510**,** 76-89.
809 DELESSERT, C., KAZAN, K., WILSON, I. W., VAN DER STRAETEN, D., MANNERS, J., DENNIS, E. S. &
810 DOLFERUS, R. 2005. The transcription factor ATAF2 represses the expression of
811 pathogenesis-related genes in Arabidopsis. *Plant J,* 43**,** 745-57.
812 DENG, Z. L., MUNCH, P. C., MRECHES, R. & MCHARDY, A. C. 2022. Rapid and accurate
813 identification of ribosomal RNA sequences via deep learning. *Nucleic Acids Res,* 50**,** e60.
814 DING, S. W., HAN, Q., WANG, J. & LI, W. X. 2018. Antiviral RNA interference in mammals. *Curr*
815 *Opin Immunol,* 54**,** 109-114.
816 DING, S. W. & VOINNET, O. 2007. Antiviral immunity directed by small RNAs. *Cell,* 130**,** 413-26.
817 DING, X. S., LIU, J., CHENG, N. H., FOLIMONOV, A., HOU, Y. M., BAO, Y., KATAGI, C., CARTER, S. A.
818 & NELSON, R. S. 2004. The Tobacco mosaic virus 126-kDa protein associated with virus
819 replication and movement suppresses RNA silencing. *Mol Plant Microbe Interact,* 17**,**
820 583-92.

821 DOS REIS FIGUEIRA, A., GOLEM, S., GOREGAOKER, S. P. & CULVER, J. N. 2002. A nuclear
822 localization signal and a membrane association domain contribute to the cellular
823 localization of the Tobacco mosaic virus 126-kDa replicase protein. *Virology,* 301**,** 81-9.
824 ERICKSON, F. L., HOLZBERG, S., CALDERON-URREA, A., HANDLEY, V., AXTELL, M., CORR, C. &
825 BAKER, B. 1999. The helicase domain of the TMV replicase proteins induces the N-
826 mediated defence response in tobacco. *Plant J,* 18**,** 67-75.
827 ESPINOZA, C., MEDINA, C., SOMERVILLE, S. & ARCE-JOHNSON, P. 2007. Senescence-associated
828 genes induced during compatible viral interactions with grapevine and Arabidopsis. *J Exp*
829 *Bot,* 58**,** 3197-212.
830 GAN, S. 2003. Mitotic and postmitotic senescence in plants. *Sci Aging Knowledge Environ,* 2003**,**
831 RE7.
832 GARCIA-RUIZ, H., TAKEDA, A., CHAPMAN, E. J., SULLIVAN, C. M., FAHLGREN, N., BREMPELIS, K. J.
833 & CARRINGTON, J. C. 2010. Arabidopsis RNA-dependent RNA polymerases and dicer-like
834 proteins in antiviral defense and small interfering RNA biogenesis during Turnip Mosaic
835 Virus infection. *Plant Cell,* 22**,** 481-96.
836 GIMENEZ-IBANEZ, S., ZAMARRENO, A. M., GARCIA-MINA, J. M. & SOLANO, R. 2019. An
837 Evolutionarily Ancient Immune System Governs the Interactions between Pseudomonas
838 syringae and an Early-Diverging Land Plant Lineage. *Curr Biol,* 29**,** 2270-2281 e4.
839 GISH, W. & STATES, D. J. 1993. Identification of protein coding regions by database similarity
840 search. *Nat Genet,* 3**,** 266-72.
841 GU, Z. 2022. Complex Heatmap Visualization. *iMeta*.
842 HERNANDEZ-GARCIA, J., BRIONES-MORENO, A. & BLAZQUEZ, M. A. 2021. Origin and evolution
843 of gibberellin signaling and metabolism in plants. *Semin Cell Dev Biol,* 109**,** 46-54.
844 HEYMAN, J., CANHER, B., BISHT, A., CHRISTIAENS, F. & DE VEYLDER, L. 2018. Emerging role of the
845 plant ERF transcription factors in coordinating wound defense responses and repair. *J*
846 *Cell Sci,* 131.
847 HOANG, D. T., CHERNOMOR, O., VON HAESELER, A., MINH, B. Q. & VINH, L. S. 2018. UFBoot2:
848 Improving the Ultrafast Bootstrap Approximation. *Molecular Biology and Evolution,* 35**,**
849 518-522.
850 HUSON, D. H., BEIER, S., FLADE, I., GÓRSKA, A., EL-HADIDI, M., MITRA, S., RUSCHEWEYH, H. J. &
851 TAPPU, R. 2016. MEGAN Community Edition - Interactive Exploration and Analysis of
852 Large-Scale Microbiome Sequencing Data. *Plos Computational Biology,* 12.
853 ISHIZAKI, K., CHIYODA, S., YAMATO, K. T. & KOHCHI, T. 2008. Agrobacterium-mediated
854 transformation of the haploid liverwort Marchantia polymorpha L., an emerging model
855 for plant biology. *Plant Cell Physiol,* 49**,** 1084-91.
856 IWAMA, R. E. & MORAN, Y. 2023. Origins and diversification of animal innate immune responses
857 against viral infections. *Nat Ecol Evol,* 7**,** 182-193.
858 JADA, B., SOITAMO, A. J., SIDDIQUI, S. A., MURUKESAN, G., ARO, E. M., SALAKOSKI, T. & LEHTO,
859 K. 2014. Multiple different defense mechanisms are activated in the young transgenic
860 tobacco plants which express the full length genome of the Tobacco mosaic virus, and
861 are resistant against this virus. *PLoS One,* 9**,** e107778.
862 JEON, H.-W., IWAKAWA, H., MARAMOTO, S., HERRFURTH, C., GUSTCHE, N., SCHLÜTER, T.,
863 KYOZUKA, J., MIYAUCHI, S., FEUSSNER, I., ZACHGO, S. & NAKAGAMI, H. 2022. Contrasting
864 and conserved roles of NPR pathways in diverged land plant lineages. *bioRxiv*.
865 JIA, X., WANG, L., ZHAO, H., ZHANG, Y., CHEN, Z., XU, L. & YI, K. 2023. The origin and evolution of
866 salicylic acid signaling and biosynthesis in plants. *Mol Plant,* 16**,** 245-259.
867 KALYAANAMOORTHY, S., MINH, B. Q., WONG, T. K. F., VON HAESELER, A. & JERMIIN, L. S. 2017.
868 ModelFinder: fast model selection for accurate phylogenetic estimates. *Nature*
869 *Methods,* 14**,** 587-+.

870 KAPPAGANTU, M., COLLUM, T. D., DARDICK, C. & CULVER, J. N. 2020. Viral Hacks of the Plant
871 Vasculature: The Role of Phloem Alterations in Systemic Virus Infection. *Annu Rev Virol,*
872 7**,** 351-370.
873 KASSCHAU, K. D., XIE, Z., ALLEN, E., LLAVE, C., CHAPMAN, E. J., KRIZAN, K. A. & CARRINGTON, J.
874 C. 2003. P1/HC-Pro, a viral suppressor of RNA silencing, interferes with Arabidopsis
875 development and miRNA unction. *Dev Cell,* 4**,** 205-17.
876 KATOH, K. & STANDLEY, D. M. 2013. MAFFT Multiple Sequence Alignment Software Version 7:
877 Improvements in Performance and Usability. *Molecular Biology and Evolution,* 30**,** 772-
878 780.
879 KNEESHAW, S., SORIANO, G., MONTE, I., HAMBERG, M., ZAMARRENO, A. M., GARCIA-MINA, J.
880 M., FRANCO-ZORRILLA, J. M., KATO, N., UEDA, M., REY-STOLLE, M. F., BARBAS, C.,
881 MICHAVILA, S., GIMENEZ-IBANEZ, S., JIMENEZ-ALEMAN, G. H. & SOLANO, R. 2022.
882 Ligand diversity contributes to the full activation of the jasmonate pathway in
883 Marchantia polymorpha. *Proc Natl Acad Sci U S A,* 119**,** e2202930119.
884 KOPYLOVA, E., NOÉ, L. & TOUZET, H. 2012. SortMeRNA: fast and accurate filtering of ribosomal
885 RNAs in metatranscriptomic data. *Bioinformatics,* 28**,** 3211-3217.
886 KORNER, C. J., KLAUSER, D., NIEHL, A., DOMINGUEZ-FERRERAS, A., CHINCHILLA, D., BOLLER, T.,
887 HEINLEIN, M. & HANN, D. R. 2013. The immunity regulator BAK1 contributes to
888 resistance against diverse RNA viruses. *Mol Plant Microbe Interact,* 26**,** 1271-80.
889 KRAMER, S. R., GOREGAOKER, S. P. & CULVER, J. N. 2011. Association of the Tobacco mosaic virus
890 126kDa replication protein with a GDI protein affects host susceptibility. *Virology,* 414**,**
891 110-8.
892 KULSHRESTHA, S., JIBRAN, R., VAN KLINK, J. W., ZHOU, Y., BRUMMELL, D. A., ALBERT, N. W.,
893 SCHWINN, K. E., CHAGNE, D., LANDI, M., BOWMAN, J. L. & DAVIES, K. M. 2022. Stress,
894 senescence, and specialized metabolites in bryophytes. *J Exp Bot,* 73**,** 4396-4411.
895 LEE, W. S., FU, S. F., LI, Z., MURPHY, A. M., DOBSON, E. A., GARLAND, L., CHALUVADI, S. R., LEWSEY,
896 M. G., NELSON, R. S. & CARR, J. P. 2016. Salicylic acid treatment and expression of an
897 RNA-dependent RNA polymerase 1 transgene inhibit lethal symptoms and meristem
898 invasion during tobacco mosaic virus infection in Nicotiana benthamiana. *BMC Plant*
899 *Biol,* 16**,** 15.
900 LEEK, J. T., JOHNSON, W. E., PARKER, H. S., FERTIG, E. J., JAFFE, A.E., ZHANG, Y., STOREY, J. D. &
901 TORRES, L. C. 2023. sva: Surrogate Variable Analysis.
902 LETUNIC, I. & BORK, P. 2021. Interactive Tree Of Life (iTOL) v5: an online tool for phylogenetic
903 tree display and annotation. *Nucleic Acids Research,* 49**,** W293-W296.
904 LEWSEY, M. G. & CARR, J. P. 2009. Effects of DICER-like proteins 2, 3 and 4 on cucumber mosaic
905 virus and tobacco mosaic virus infections in salicylic acid-treated plants. *J Gen Virol,* 90**,**
906 3010-3014.
907 LIANG, Y., HEYMAN, J., XIANG, Y., VANDENDRIESSCHE, W., CANHER, B., GOEMINNE, G. & DE
908 VEYLDER, L. 2022. The wound-activated ERF15 transcription factor drives Marchantia
909 polymorpha regeneration by activating an oxylipin biosynthesis feedback loop. *Sci Adv,*
910 8**,** eabo7737.
911 LIM, P. O. & NAM, H. G. 2005. The molecular and genetic control of leaf senescence and longevity
912 in Arabidopsis. *Curr Top Dev Biol,* 67**,** 49-83.
913 LIU, C. & NELSON, R. S. 2013. The cell biology of Tobacco mosaic virus replication and movement.
914 *Front Plant Sci,* 4**,** 12.
915 LIU, Y., GAO, Q., WU, B., AI, T. & GUO, X. 2009. NgRDR1, an RNA-dependent RNA polymerase
916 isolated from Nicotiana glutinosa, was involved in biotic and abiotic stresses. *Plant*
917 *Physiol Biochem,* 47**,** 359-68.

LOPEZ-GOMOLLON, S. & BAULCOMBE, D. C. 2022. Roles of RNA silencing in viral and non-viral plant immunity and in the crosstalk between disease resistance systems. *Nat Rev Mol Cell Biol,* 23**,** 645-662.

LOVE, M. I., HUBER, W. & ANDERS, S. 2014. Moderated estimation of fold change and dispersion for RNA-seq data with DESeq2. *Genome Biol,* 15**,** 550.

LUCAS, W. J., GROOVER, A., LICHTENBERGER, R., FURUTA, K., YADAV, S. R., HELARIUTTA, Y., HE, X. Q., FUKUDA, H., KANG, J., BRADY, S. M., PATRICK, J. W., SPERRY, J., YOSHIDA, A., LOPEZ-MILLAN, A. F., GRUSAK, M. A. & KACHROO, P. 2013. The plant vascular system: evolution, development and functions. *J Integr Plant Biol,* 55**,** 294-388.

MANDADI, K. K. & SCHOLTHOF, K. B. 2013. Plant immune responses against viruses: how does a virus cause disease? *Plant Cell,* 25**,** 1489-505.

MATSUI, H., IWAKAWA, H., HYON, G. S., YOTSUI, I., KATOU, S., MONTE, I., NISHIHAMA, R., FRANZEN, R., SOLANO, R. & NAKAGAMI, H. 2020. Isolation of Natural Fungal Pathogens from Marchantia polymorpha Reveals Antagonism between Salicylic Acid and Jasmonate during Liverwort-Fungus Interactions. *Plant Cell Physiol,* 61**,** 265-275.

MONTE, I., FRANCO-ZORRILLA, J. M., GARCIA-CASADO, G., ZAMARRENO, A. M., GARCIA-MINA, J. M., NISHIHAMA, R., KOHCHI, T. & SOLANO, R. 2019. A Single JAZ Repressor Controls the Jasmonate Pathway in Marchantia polymorpha. *Mol Plant,* 12**,** 185-198.

MONTE, I., ISHIDA, S., ZAMARRENO, A. M., HAMBERG, M., FRANCO-ZORRILLA, J. M., GARCIA-CASADO, G., GOUHIER-DARIMONT, C., REYMOND, P., TAKAHASHI, K., GARCIA-MINA, J. M., NISHIHAMA, R., KOHCHI, T. & SOLANO, R. 2018. Ligand-receptor co-evolution shaped the jasmonate pathway in land plants. *Nat Chem Biol,* 14**,** 480-488.

MUSHEGIAN, A., SHIPUNOV, A. & ELENA, S. F. 2016. Changes in the composition of the RNA virome mark evolutionary transitions in green plants. *BMC Biol,* 14**,** 68.

NGUYEN, L. T., SCHMIDT, H. A., VON HAESELER, A. & MINH, B. Q. 2015. IQ-TREE: A Fast and Effective Stochastic Algorithm for Estimating Maximum-Likelihood Phylogenies. *Molecular Biology and Evolution,* 32**,** 268-274.

NIEHL, A., WYRSCH, I., BOLLER, T. & HEINLEIN, M. 2016. Double-stranded RNAs induce a pattern-triggered immune signaling pathway in plants. *New Phytol,* 211**,** 1008-19.

PATRO, R., DUGGAL, G., LOVE, M. I., IRIZARRY, R. A. & KINGSFORD, C. 2017. Salmon provides fast and bias-aware quantification of transcript expression. *Nature Methods,* 14**,** 417-+.

PEART, J. R., COOK, G., FEYS, B. J., PARKER, J. E. & BAULCOMBE, D. C. 2002. An EDS1 orthologue is required for N-mediated resistance against tobacco mosaic virus. *Plant J,* 29**,** 569-79.

PRUITT, R. N., LOCCI, F., WANKE, F., ZHANG, L., SAILE, S. C., JOE, A., KARELINA, D., HUA, C., FROHLICH, K., WAN, W. L., HU, M., RAO, S., STOLZE, S. C., HARZEN, A., GUST, A. A., HARTER, K., JOOSTEN, M., THOMMA, B., ZHOU, J. M., DANGL, J. L., WEIGEL, D., NAKAGAMI, H., OECKING, C., KASMI, F. E., PARKER, J. E. & NURNBERGER, T. 2021. The EDS1-PAD4-ADR1 node mediates Arabidopsis pattern-triggered immunity. *Nature,* 598**,** 495-499.

QUILLIAM, R. S., SWARBRICK, P. J., SCHOLES, J. D. & ROLFE, S. A. 2006. Imaging photosynthesis in wounded leaves of Arabidopsis thaliana. *J Exp Bot,* 57**,** 55-69.

RAKHSHANDEHROO, F., REZAEE, S. & PALUKAITIS, P. 2017. Silencing the tobacco gene for RNA-dependent RNA polymerase 1 and infection by potato virus Y cause remodeling of cellular organelles. *Virology,* 510**,** 127-136.

REDKAR, A., GIMENEZ IBANEZ, S., SABALE, M., ZECHMANN, B., SOLANO, R. & DI PIETRO, A. 2022. Marchantia polymorpha model reveals conserved infection mechanisms in the vascular wilt fungal pathogen Fusarium oxysporum. *New Phytol,* 234**,** 227-241.

SALGUERO-LINARES, J., SERRANO, I., RUIZ-SOLANI, N., SALAS-GOMEZ, M., PHUKAN, U. J., GONZALEZ, V. M., BERNARDO-FAURA, M., VALLS, M., RENGEL, D. & COLL, N. S. 2022.

967 Robust transcriptional indicators of immune cell death revealed by spatiotemporal
968 transcriptome analyses. *Mol Plant,* 15**,** 1059-1075.
969 SCHINDELIN, J., ARGANDA-CARRERAS, I., FRISE, E., KAYNIG, V., LONGAIR, M., PIETZSCH, T.,
970 PREIBISCH, S., RUEDEN, C., SAALFELD, S., SCHMID, B., TINEVEZ, J. Y., WHITE, D. J.,
971 HARTENSTEIN, V., ELICEIRI, K., TOMANCAK, P. & CARDONA, A. 2012. Fiji: an open-source
972 platform for biological-image analysis. *Nat Methods,* 9**,** 676-82.
973 SCHOLTHOF, K. B. 2004. Tobacco mosaic virus: a model system for plant biology. *Annu Rev*
974 *Phytopathol,* 42**,** 13-34.
975 SCHOMMER, C., PALATNIK, J. F., AGGARWAL, P., CHETELAT, A., CUBAS, P., FARMER, E. E., NATH,
976 U. & WEIGEL, D. 2008. Control of jasmonate biosynthesis and senescence by miR319
977 targets. *PLoS Biol,* 6**,** e230.
978 SCHWACH, F., VAISTIJ, F. E., JONES, L. & BAULCOMBE, D. C. 2005. An RNA-dependent RNA
979 polymerase prevents meristem invasion by potato virus X and is required for the activity
980 but not the production of a systemic silencing signal. *Plant Physiol,* 138**,** 1842-52.
981 SHENG, Y., YANG, L., LI, C., WANG, Y. & GUO, H. 2019. Transcriptomic changes in Nicotiana
982 tabacum leaves during mosaic virus infection. *3 Biotech,* 9**,** 220.
983 SONESON, C., LOVE, M. I. & ROBINSON, M. D. 2015. Differential analyses for RNA-seq: transcript-
984 level estimates improve gene-level inferences. *F1000Res,* 4**,** 1521.
985 VASSEUR, F., BALDRICH, P., JIMENEZ-GONGORA, T., VILLAR-MARTIN, L., WEIGEL, D. & RUBIO-
986 SOMOZA, I. 2022. miRNA472 deficiency enhances Arabidopsis thaliana defence without
987 reducing seed production. *bioRxiv,* doi.org/10.1101/2022.12.13.520224
988 WANG, L., WAN, M. C., LIAO, R. Y., XU, J., XU, Z. G., XUE, H. C., MAI, Y. X. & WANG, J. W. 2023. The
989 maturation and aging trajectory of Marchantia polymorpha at single-cell resolution. *Dev*
990 *Cell,* 58**,** 1429-1444 e6.
991 WANG, X., GOREGAOKER, S. P. & CULVER, J. N. 2009. Interaction of the Tobacco mosaic virus
992 replicase protein with a NAC domain transcription factor is associated with the
993 suppression of systemic host defenses. *J Virol,* 83**,** 9720-30.
994 WHITHAM, S., DINESH-KUMAR, S. P., CHOI, D., HEHL, R., CORR, C. & BAKER, B. 1994. The product
995 of the tobacco mosaic virus resistance gene N: similarity to toll and the interleukin-1
996 receptor. *Cell,* 78**,** 1101-15.
997 XU, T., ZHANG, L., ZHEN, J., FAN, Y., ZHANG, C. & WANG, L. 2013. Expressional and regulatory
998 characterization of Arabidopsis RNA-dependent RNA polymerase 1. *Planta,* 237**,** 1561-9.
999 YAMANAKA, T., OHTA, T., TAKAHASHI, M., MESHI, T., SCHMIDT, R., DEAN, C., NAITO, S. &
1000 ISHIKAWA, M. 2000. TOM1, an Arabidopsis gene required for efficient multiplication of
1001 a tobamovirus, encodes a putative transmembrane protein. *Proc Natl Acad Sci U S A,* 97**,**
1002 10107-12.
1003 YING, X. B., DONG, L., ZHU, H., DUAN, C. G., DU, Q. S., LV, D. Q., FANG, Y. Y., GARCIA, J. A., FANG,
1004 R. X. & GUO, H. S. 2010. RNA-dependent RNA polymerase 1 from Nicotiana tabacum
1005 suppresses RNA silencing and enhances viral infection in Nicotiana benthamiana. *Plant*
1006 *Cell,* 22**,** 1358-72.
1007 YOTSUI, I., MATSUI, H., MIYAUCHI, S., IWAKAWA, H., MELKONIAN, K., SCHLUTER, T., MICHAVILA,
1008 S., KANAZAWA, T., NOMURA, Y., STOLZE, S. C., JEON, H. W., YAN, Y., HARZEN, A., SUGANO,
1009 S. S., SHIRAKAWA, M., NISHIHAMA, R., ICHIHASHI, Y., IBANEZ, S. G., SHIRASU, K., UEDA,
1010 T., KOHCHI, T. & NAKAGAMI, H. 2023. LysM-mediated signaling in Marchantia
1011 polymorpha highlights the conservation of pattern-triggered immunity in land plants.
1012 *Curr Biol,* 33**,** 3732-3746 e8.
1013 YU, D., FAN, B., MACFARLANE, S. A. & CHEN, Z. 2003. Analysis of the involvement of an inducible
1014 Arabidopsis RNA-dependent RNA polymerase in antiviral defense. *Mol Plant Microbe*
1015 *Interact,* 16**,** 206-16.

1016 YU, X., XU, Y. & YAN, S. 2021. Salicylic acid and ethylene coordinately promote leaf senescence. *J*
1017 *Integr Plant Biol,* 63**,** 823-827.
1018 ZHU, F., XI, D. H., YUAN, S., XU, F., ZHANG, D. W. & LIN, H. H. 2014. Salicylic acid and jasmonic
1019 acid are essential for systemic resistance against tobacco mosaic virus in Nicotiana
1020 benthamiana. *Mol Plant Microbe Interact,* 27**,** 567-77.

1021

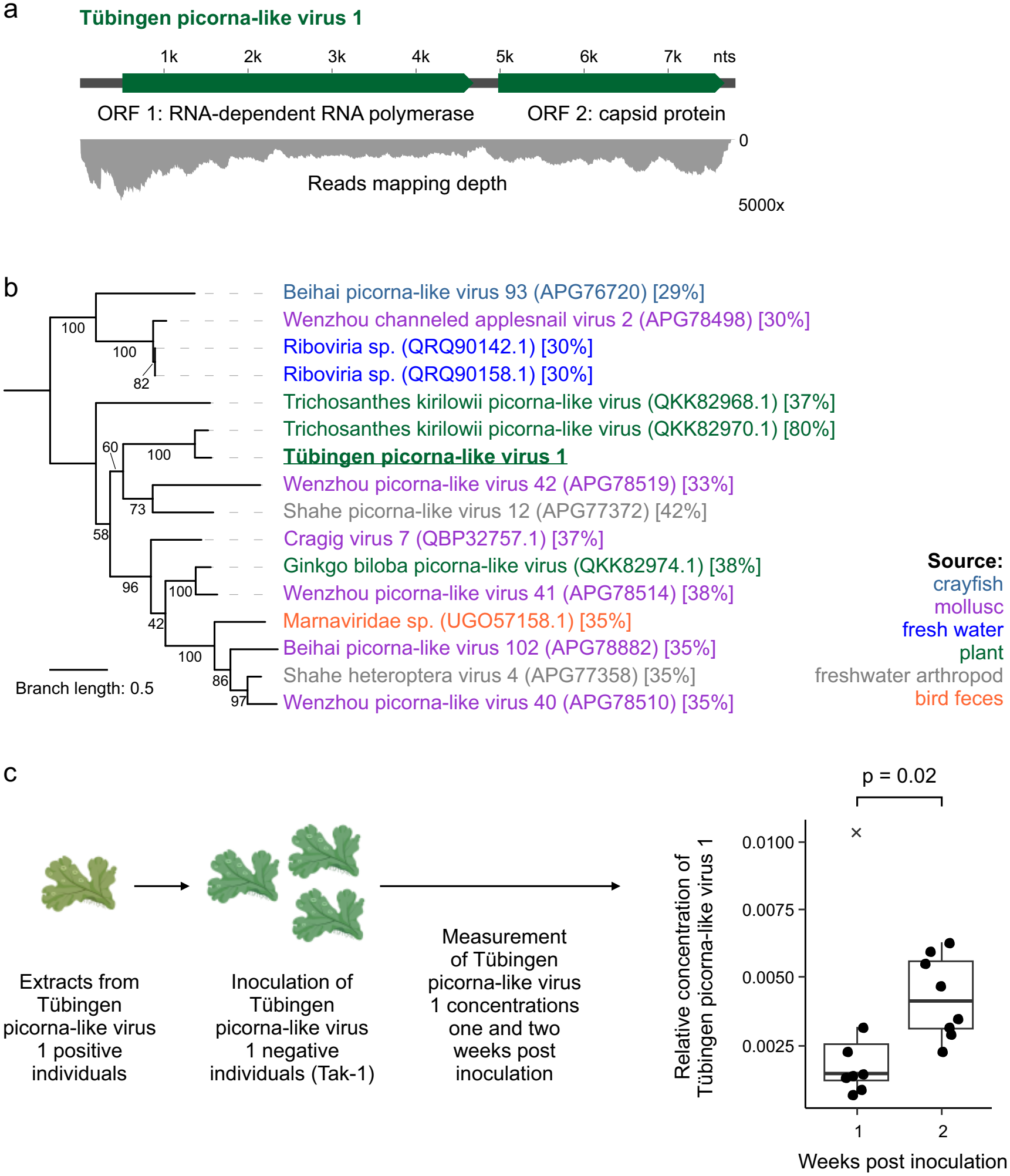
a
Tübingen picorna-like virus 1
1k
2k
3k
4k
5k
6k
7k
nts
ORF 1: RNA-dependent RNA polymerase
ORF 2: capsid protein
0
Reads mapping depth
5000x
b
Beihai picorna-like virus 93 (APG76720) [29%]
Wenzhou channeled applesnail virus 2 (APG78498) [30%]
Riboviria sp. (QRQ90142.1) [30%]
Riboviria sp. (QRQ90158.1) [30%]
Trichosanthes kirilowii picorna-like virus (QKK82968.1) [37%]
Trichosanthes kirilowii picorna-like virus (QKK82970.1) [80%]
Tübingen picorna-like virus 1
Wenzhou picorna-like virus 42 (APG78519) [33%]
Shahe picorna-like virus 12 (APG77372) [42%]
Cragig virus 7 (QBP32757.1) [37%]
Ginkgo biloba picorna-like virus (QKK82974.1) [38%]
Wenzhou picorna-like virus 41 (APG78514) [38%]
Marnaviridae sp. (UGO57158.1) [35%]
Beihai picorna-like virus 102 (APG78882) [35%]
Shahe heteroptera virus 4 (APG77358) [35%]
Wenzhou picorna-like virus 40 (APG78510) [35%]
100
100
82
60
100
73
58
96
100
42
100
86
97
Branch length: 0.5
Source:
crayfish
mollusc
fresh water
plant
freshwater arthropod
bird feces
c
Extracts from Tübingen picorna-like virus 1 positive individuals
Inoculation of Tübingen picorna-like virus 1 negative individuals (Tak-1)
Measurement of Tübingen picorna-like virus 1 concentrations one and two weeks post inoculation
p = 0.02
Relative concentration of Tübingen picorna-like virus 1
0.0100
0.0075
0.0050
0.0025
1
2
Weeks post inoculation

A

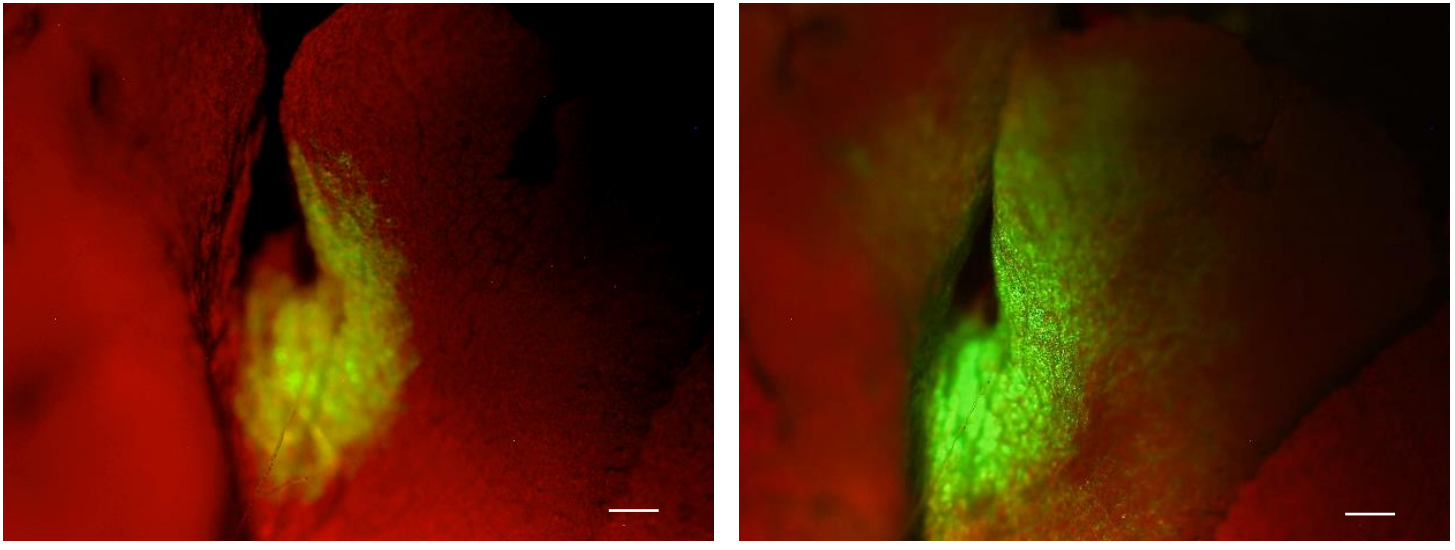

B

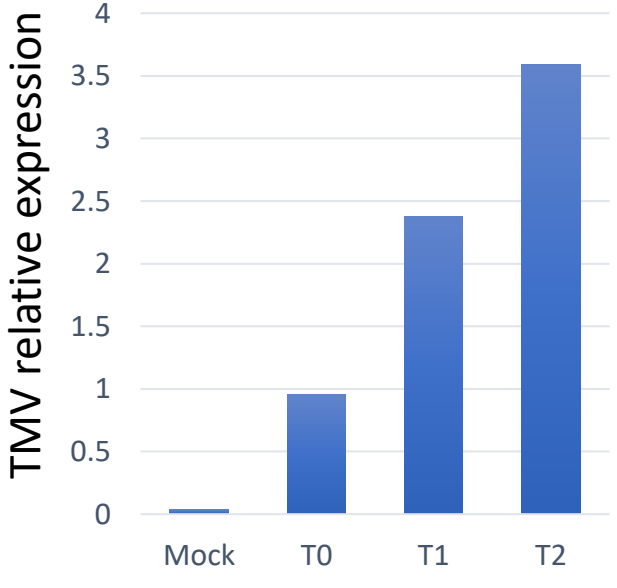

C

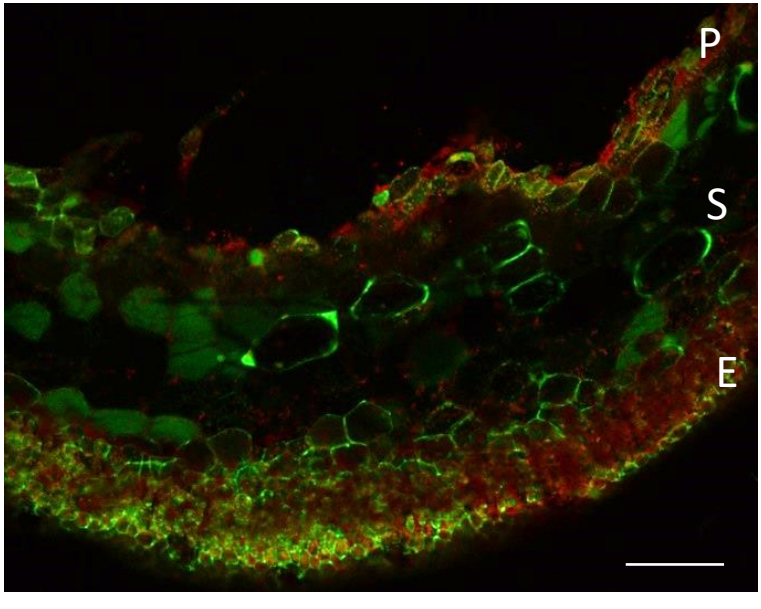

A

Name	ID	Relative expression level
MpPR9	Mp521510	4.04
MpSYP13B	Mp2g21910	2.34
MpCML42	Mp6g18000	1.79
MpWRKY22	Mp7g17200	1.74
MpACRE132	Mp1g27170	1.22

B

Name	ID	Relative expression level
MpERF1	Mp7g09350	4.24
MpERF16	Mp4g22290	3.11
MpERF10	Mp7g00860	2.83
MpERF21	Mp5g22160	1.68
MpERF8	Mp6g18650	1.48
MpERF18	Mp5g12480	1.14
MpERF15	Mp7g09350	1.06
MpAP2L1	Mp8g11450	-1.62
MpERF17	Mp4g22280	-2.38
MpERF12	Mp6g06870	-2.95
MpERF13	Mp6g08690	-3.25

C

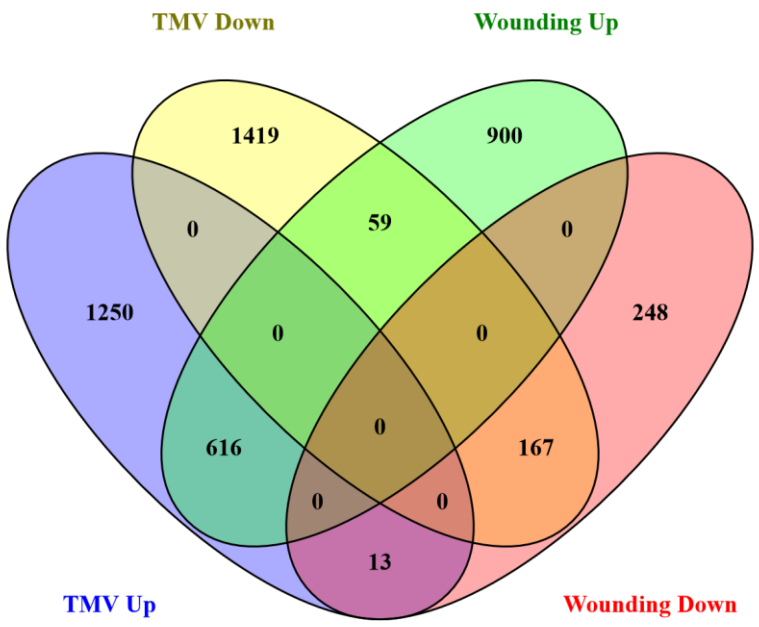

D

Name	ID	Relative expression level
MpWRKY7	Mp3g17660	3.56
MpWRKY6	Mp1g08960	2.52
MpWRKY12	Mp4g00200	1.89
MpWRKY10	Mp7g06550	1.79
MpWRKY9	Mp7g17200	1.74
MpWRKY13	Mp4g00180	1.64
MpWRKY1	Mp7g00010	1.28
MpWRKY14	Mp6g16800	1.16

E

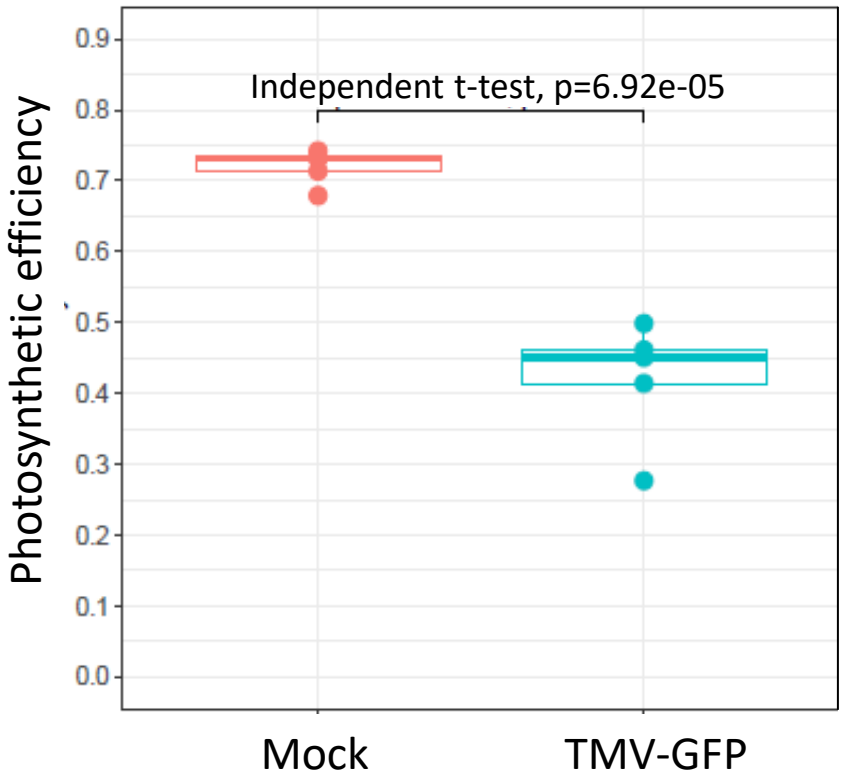

F

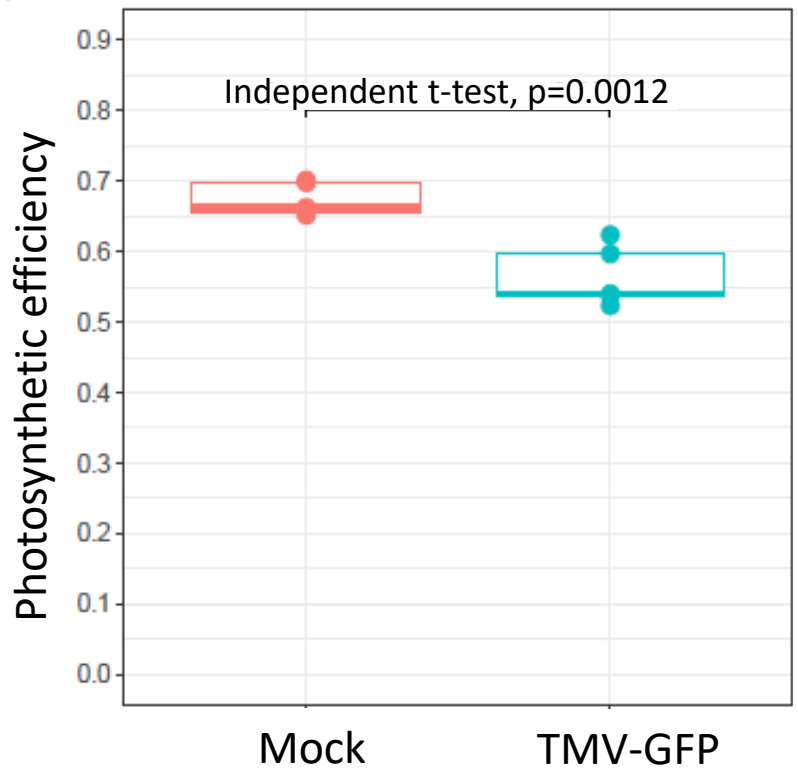

G

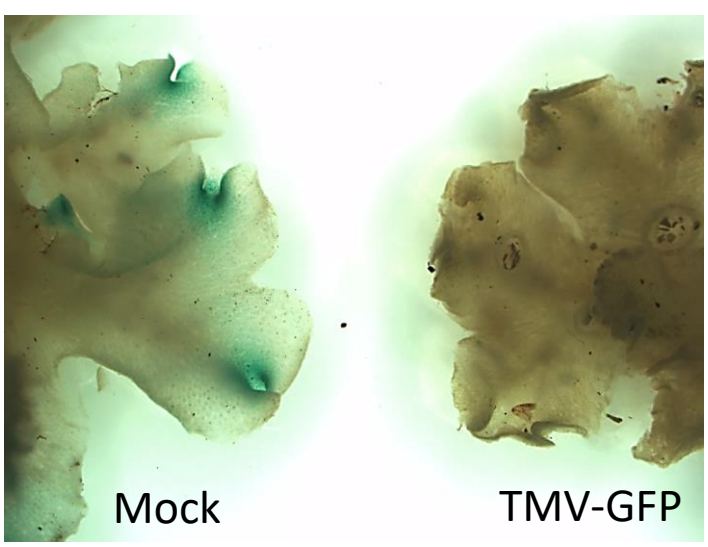

A

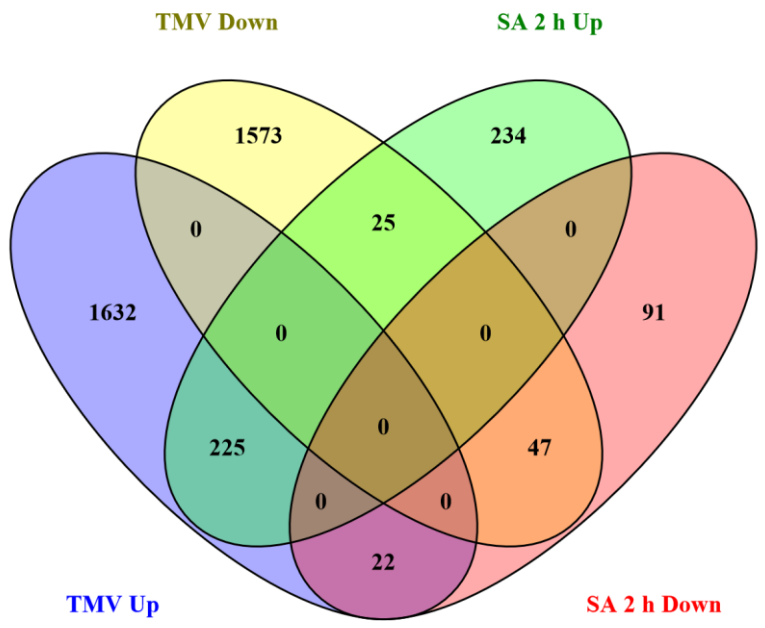
TMV Down
SA 2 h Up
1573
234
0
25
0
1632
0
0
91
225
0
47
0
0
22
TMV Up
SA 2 h Down

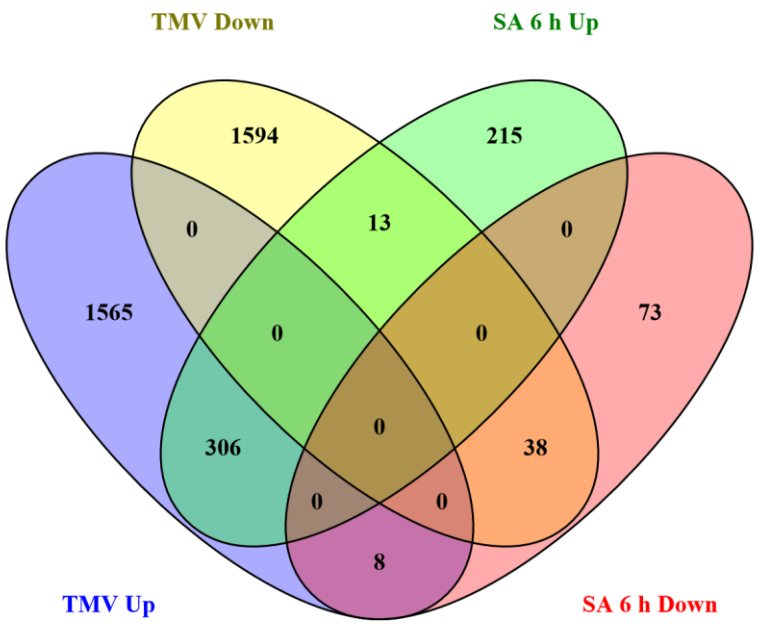
TMV Down
SA 6 h Up
1594
215
0
13
0
1565
0
0
73
306
0
38
0
0
8
TMV Up
SA 6 h Down

B

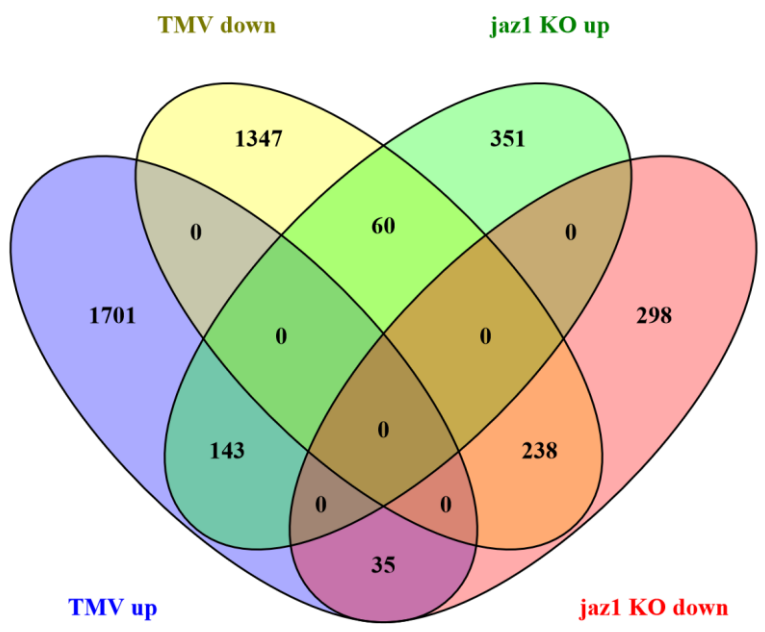
TMV down
jaz1 KO up
1347
351
0
60
0
1701
0
0
298
143
0
238
0
0
35
TMV up
jaz1 KO down

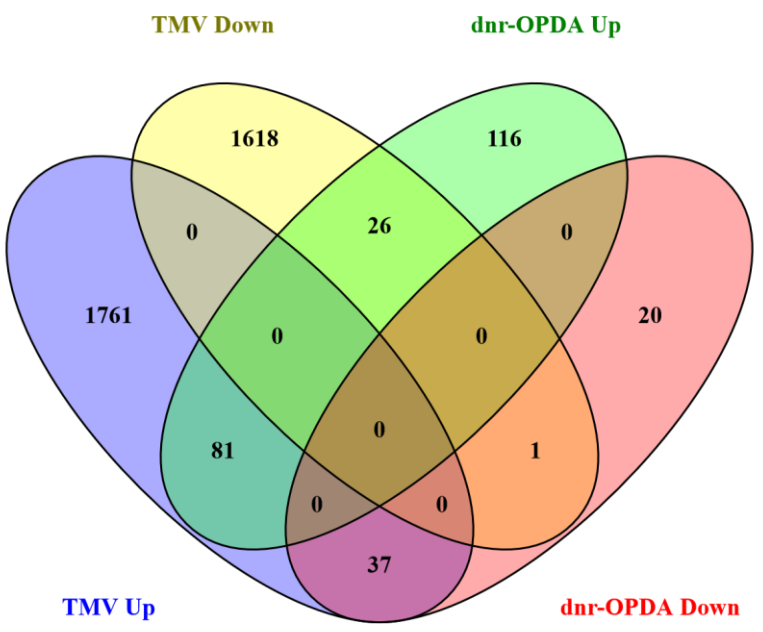
TMV Down
dnr-OPDA Up
1618
116
0
26
0
1761
0
0
20
81
0
1
0
0
37
TMV Up
dnr-OPDA Down

C

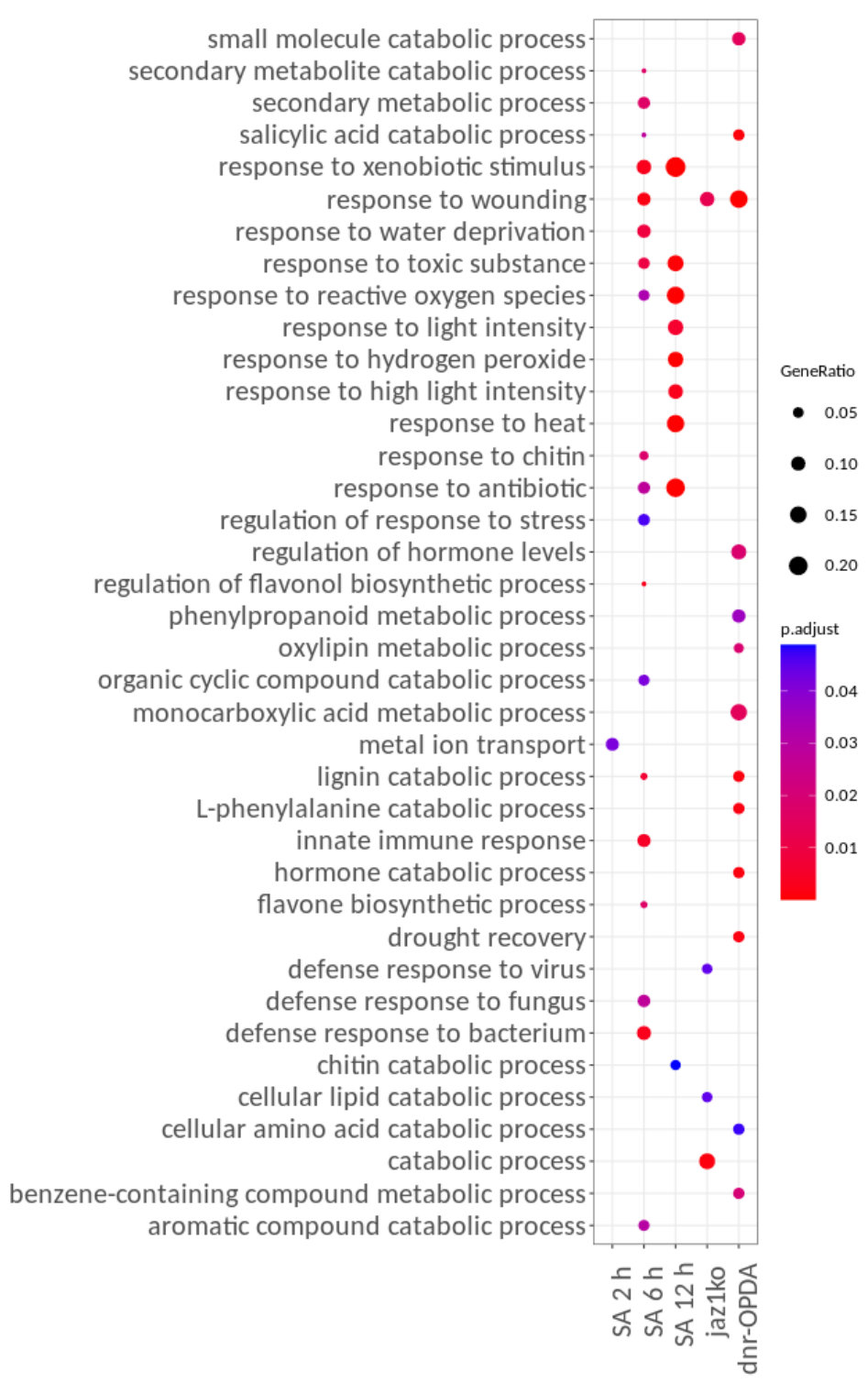
small molecule catabolic process
secondary metabolite catabolic process
secondary metabolic process
salicylic acid catabolic process
response to xenobiotic stimulus
response to wounding
response to water deprivation
response to toxic substance
response to reactive oxygen species
response to light intensity
response to hydrogen peroxide
response to high light intensity
response to heat
response to chitin
response to antibiotic
regulation of response to stress
regulation of hormone levels
regulation of flavonol biosynthetic process
phenylpropanoid metabolic process
oxylipin metabolic process
organic cyclic compound catabolic process
monocarboxylic acid metabolic process
metal ion transport
lignin catabolic process
L-phenylalanine catabolic process
innate immune response
hormone catabolic process
flavone biosynthetic process
drought recovery
defense response to virus
defense response to fungus
defense response to bacterium
chitin catabolic process
cellular lipid catabolic process
cellular amino acid catabolic process
catabolic process
benzene-containing compound metabolic process
aromatic compound catabolic process
SA 2 h
SA 6 h
SA 12 h
jaz1ko
dnr-OPDA
GeneRatio
0.05
0.10
0.15
0.20
p.adjust
0.04
0.03
0.02
0.01

D

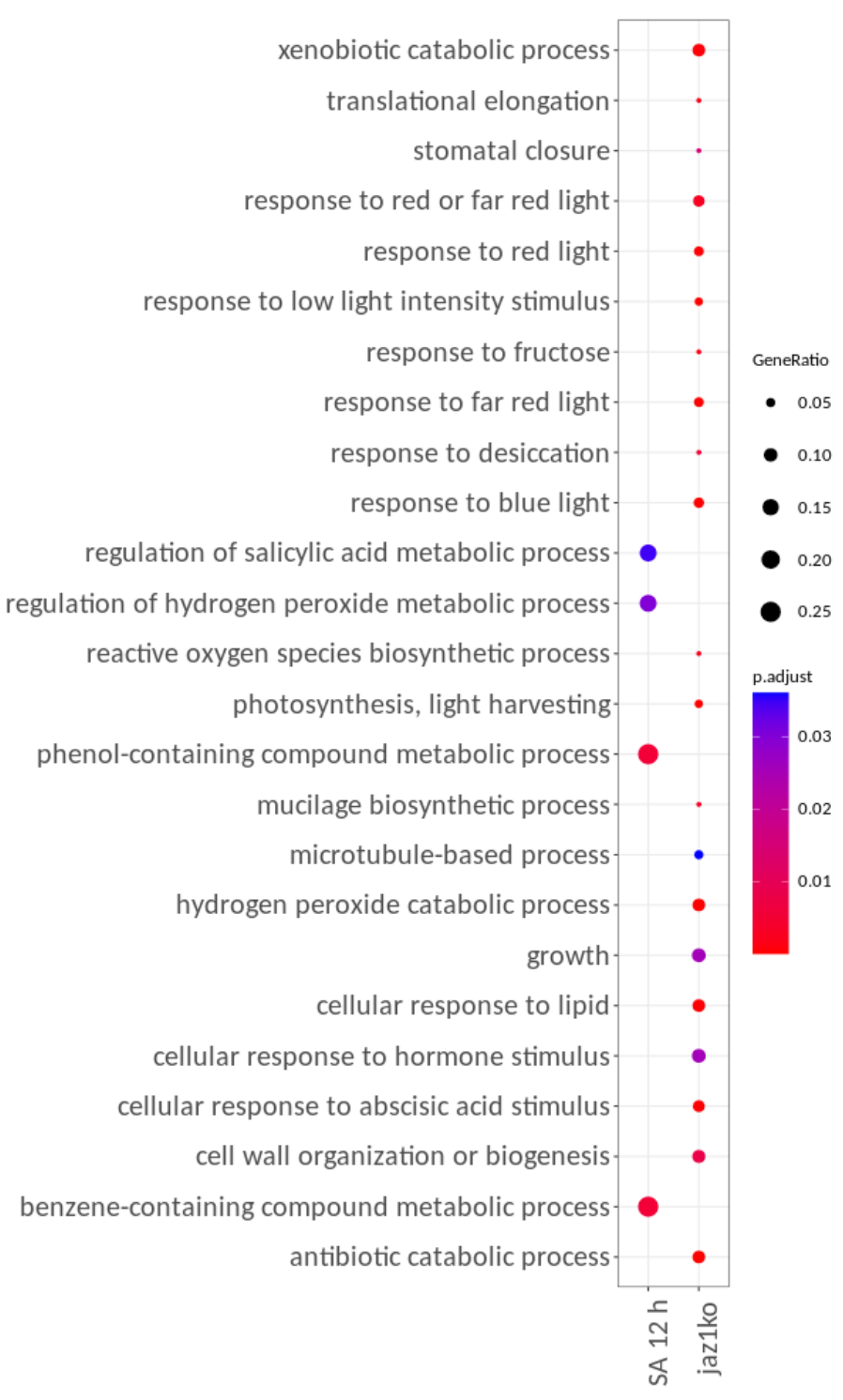
xenobiotic catabolic process
translational elongation
stomatal closure
response to red or far red light
response to red light
response to low light intensity stimulus
response to fructose
response to far red light
response to desiccation
response to blue light
regulation of salicylic acid metabolic process
regulation of hydrogen peroxide metabolic process
reactive oxygen species biosynthetic process
photosynthesis, light harvesting
phenol-containing compound metabolic process
mucilage biosynthetic process
microtubule-based process
hydrogen peroxide catabolic process
growth
cellular response to lipid
cellular response to hormone stimulus
cellular response to abscisic acid stimulus
cell wall organization or biogenesis
benzene-containing compound metabolic process
antibiotic catabolic process
SA 12 h
jaz1ko
GeneRatio
0.05
0.10
0.15
0.20
0.25
p.adjust
0.03
0.02
0.01

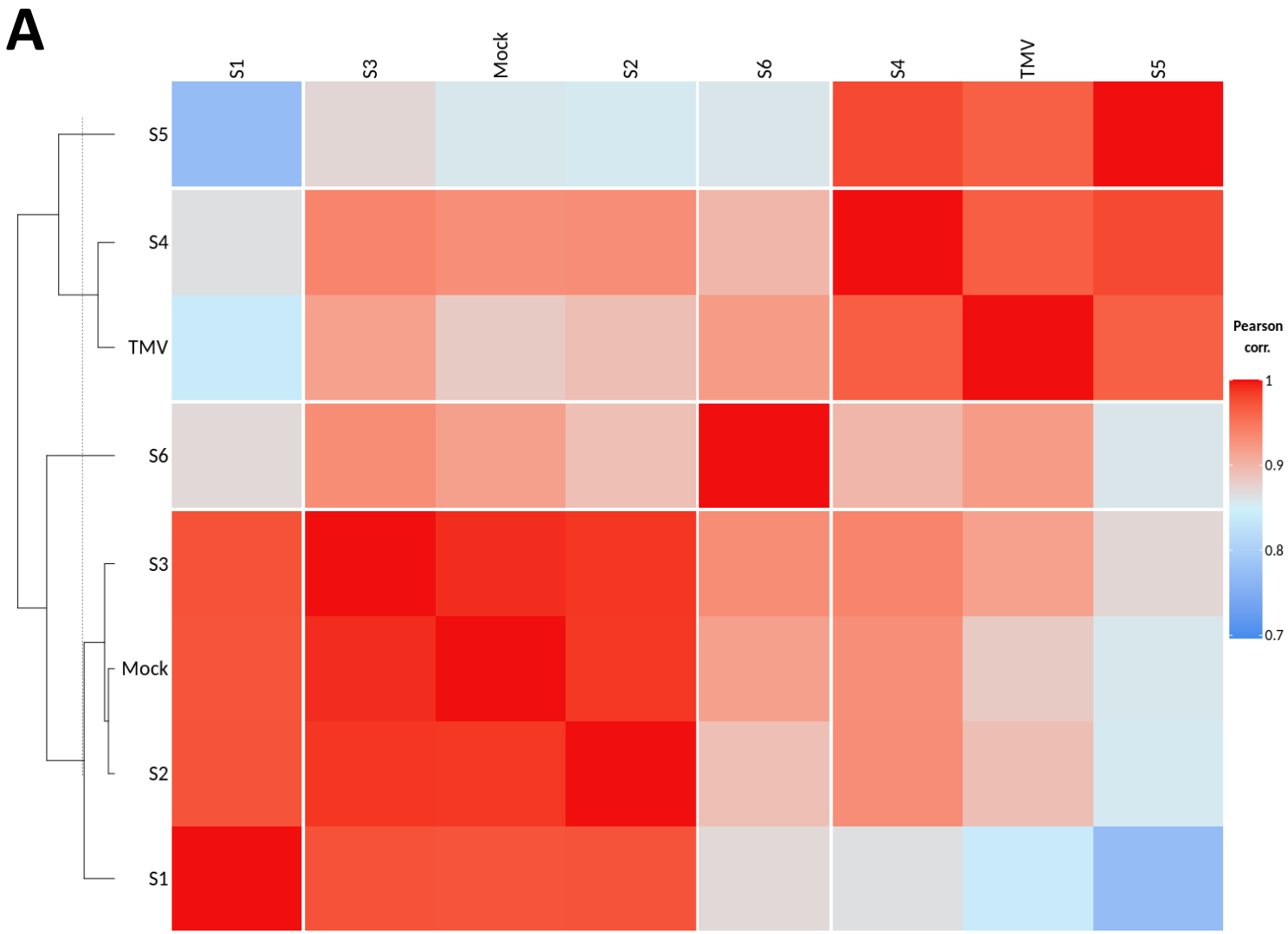
A
S1
S3
Mock
S2
S6
S4
TMV
S5
S5
S4
TMV
S6
S3
Mock
S2
S1
Pearson corr.
1
0.9
0.8
0.7

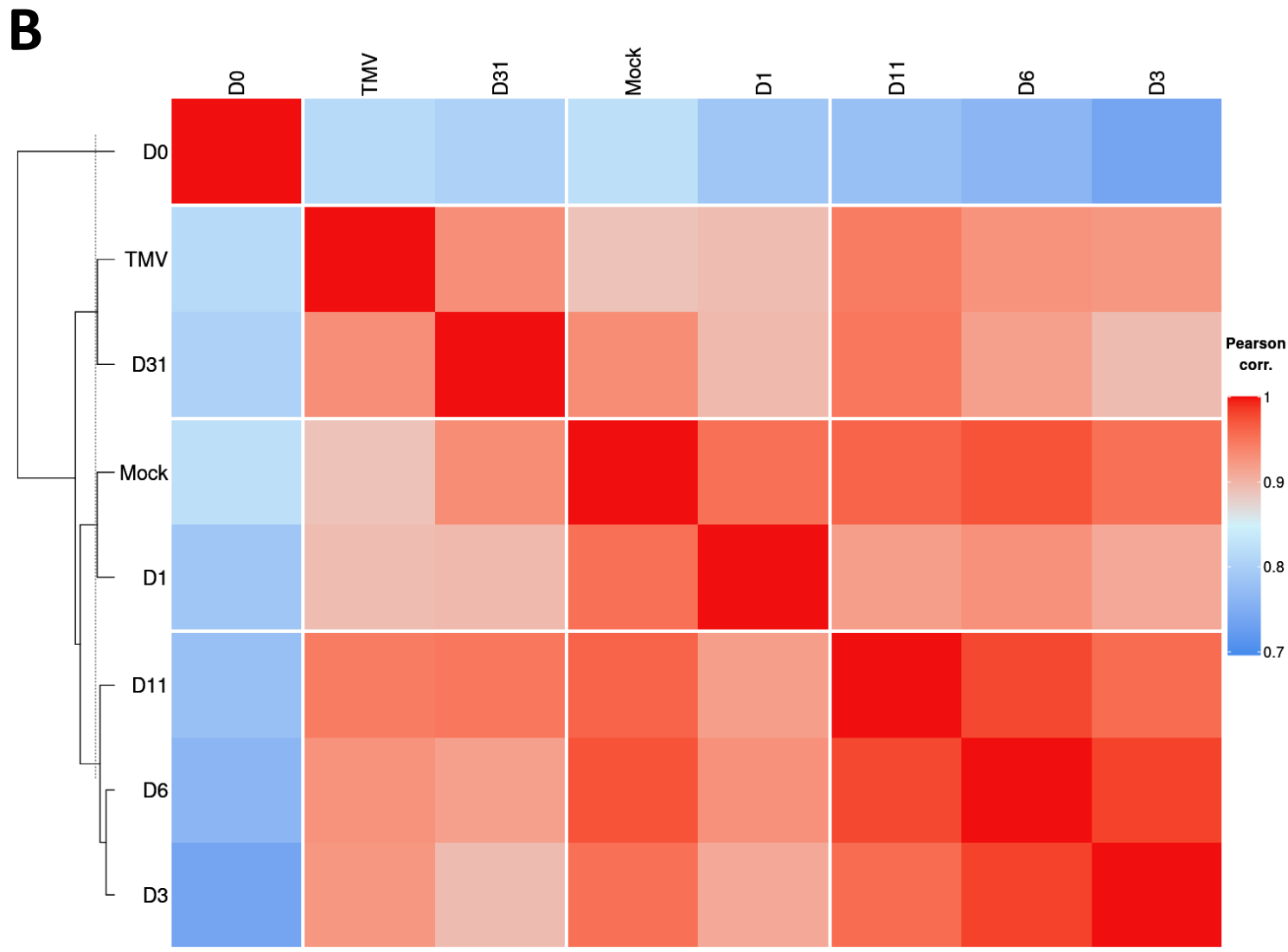
B
D0
TMV
D31
Mock
D1
D11
D6
D3
D0
TMV
D31
Mock
D1
D11
D6
D3
Pearson corr.
1
0.9
0.8
0.7

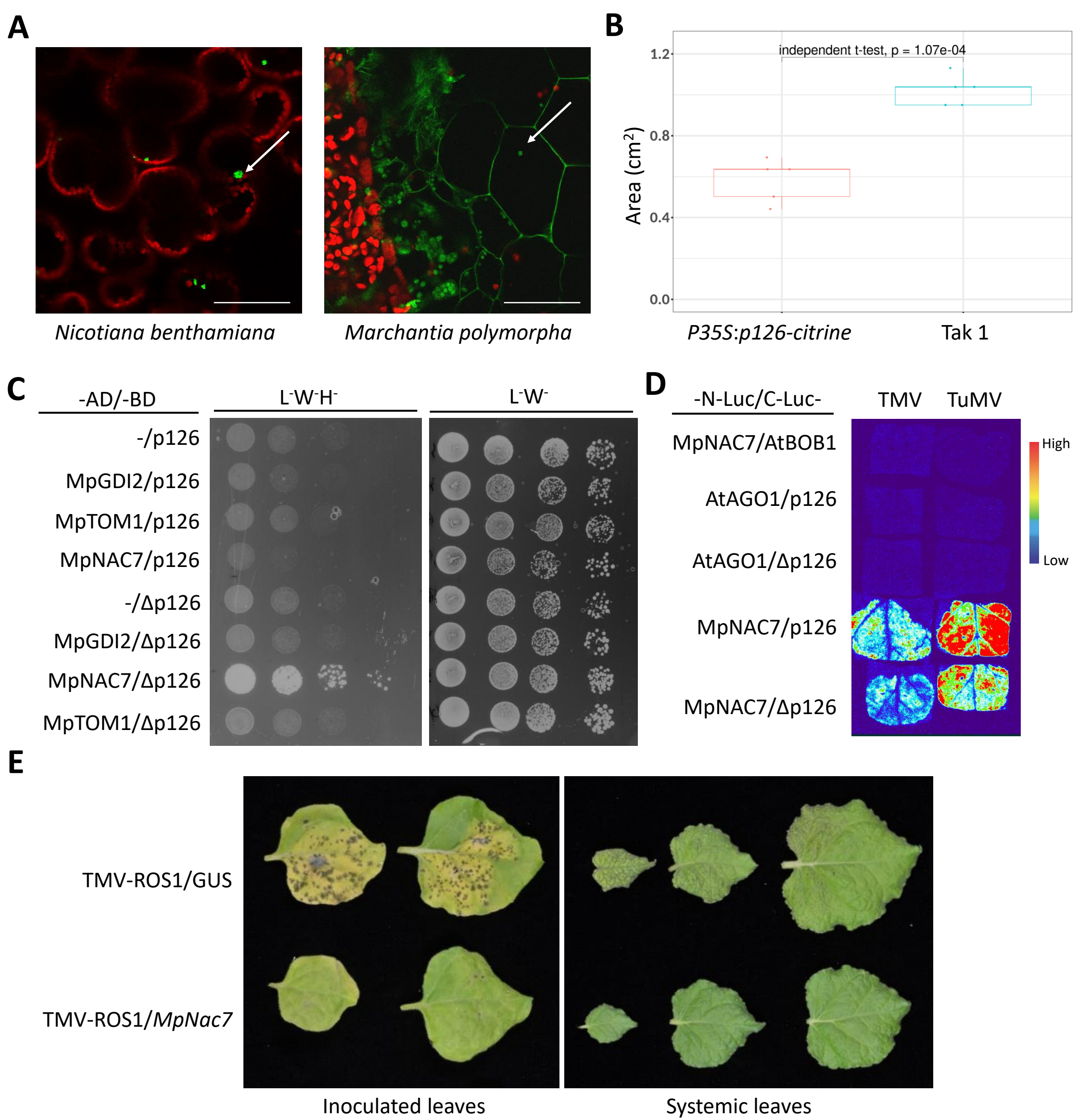
A
Nicotiana benthamiana
Marchantia polymorpha
B
independent t-test, p = 1.07e-04
Area (cm²)
1.2
0.8
0.4
0.0
P35S:p126-citrine
Tak 1
C
-AD/-BD
L⁻W⁻H⁻
L⁻W⁻
-/p126
MpGDI2/p126
MpTOM1/p126
MpNAC7/p126
-/Δp126
MpGDI2/Δp126
MpNAC7/Δp126
MpTOM1/Δp126
D
-N-Luc/C-Luc-
TMV
TuMV
MpNAC7/AtBOB1
AtAGO1/p126
AtAGO1/Δp126
MpNAC7/p126
MpNAC7/Δp126
High
Low
E
TMV-ROS1/GUS
TMV-ROS1/MpNac7
Inoculated leaves
Systemic leaves